MARTIN MARIETTA ENERGY SYSTEMS LIBRARIES
3 4456 0364507 2

77

ORNL-3261, Suppl.
UC-80 – Reactor Technology

LIFETIME STUDIES FOR THE N.S. SAVANNAH REACTOR

E. E. Gross
M. L. Winton
B. W. Colston

CENTRAL RESEARCH LIBRARY
DOCUMENT COLLECTION
LIBRARY LOAN COPY
DO NOT TRANSFER TO ANOTHER PERSON
If you wish someone else to see this document, send in name with document and the library will arrange a loan.

OAK RIDGE NATIONAL LABORATORY
operated by
UNION CARBIDE CORPORATION
for the
U.S. ATOMIC ENERGY COMMISSION

Printed in USA. Price: $1.00 Available from the
Office of Technical Services
U. S. Department of Commerce
Washington 25, D. C.

LEGAL NOTICE

This report was prepared as an account of Government sponsored work. Neither the United States, nor the Commission, nor any person acting on behalf of the Commission:

A. Makes any warranty or representation, expressed or implied, with respect to the accuracy, completeness, or usefulness of the information contained in this report, or that the use of any information, apparatus, method, or process disclosed in this report may not infringe privately owned rights; or

B. Assumes any liabilities with respect to the use of, or for damages resulting from the use of any information, apparatus, method, or process disclosed in this report.

As used in the above, "person acting on behalf of the Commission" includes any employee or contractor of the Commission, or employee of such contractor, to the extent that such employee or contractor of the Commission, or employee of such contractor prepares, disseminates, or provides access to, any information pursuant to his employment or contract with the Commission, or his employment with such contractor.

ORNL-3261, Suppl.

Contract No. W-7405-eng-26

Reactor Division

LIFETIME STUDIES FOR THE N.S. SAVANNAH REACTOR

E. E. Gross M. L. Winton
B. W. Colston

Date Issued

MAR 18 1963

OAK RIDGE NATIONAL LABORATORY
Oak Ridge, Tennessee
operated by
UNION CARBIDE CORPORATION
for the
U. S. ATOMIC ENERGY COMMISSION

MARTIN MARIETTA ENERGY SYSTEMS LIBRARIES
3 4456 0364507 2

CONTENTS

ABSTRACT v

1. INTRODUCTION 1

2. DESCRIPTION OF THE CORE 2

3. BEGINNING-OF-LIFE CORE ANALYSIS 5

4. BURNUP ANALYSIS 9

Analytical Model 9

Geometry and Initial Conditions 11

Radial Burnup 11

Axial Burnup 12

Cross Sections and Bucklings 15

5. COMPARISON OF ONE- AND TWO-ZONE CORE REACTIVITY LIFETIMES 18

6. EFFECT OF FISSION-PRODUCT NONTHERMAL ABSORPTIONS OF REACTIVITY LIFETIME 23

7. INVESTIGATION OF FUEL-RESHUFFLING SCHEMES 24

8. COMPARISON OF AXIAL SLAB-GEOMETRY MODEL WITH EXPERIMENT 26

9. COMPARISON OF RADIAL AND WINDOW-SHADE BURNUP METHODS FOR N.S. SAVANNAH CORE I CALCULATIONS 27

Radial-Burnup Lifetime Results 27

Window-Shade-Burnup Lifetime Results 27

Axial Power Distributions 30

10. WINDOW-SHADE BURNUP RESULTS FOR 4.2-WT % ENRICHED ZIRCALOY EGG-CRATE CORE 31

Core Life 31

Axial Power Distributions 33

11. TEMPERATURE COEFFICIENT OF REACTIVITY 34

Acknowledgment 35

REFERENCES 36

ABSTRACT

Previous studies of the N.S. SAVANNAH core I reactor were extended by a series of one-dimensional lifetime calculations to investigate several questions of interest in the operation of the reactor.

Replacement of the actual two-zone loading by a single-zone loading with the inner-zone enrichment was found to have only a small effect on the calculated reactivity lifetime. The time-dependent core inventories of U^{235}, Pu^{239}, and Pu^{241} for core I were calculated.

Various fuel-management schemes for extending the reactivity lifetime of core I were investigated, and the data showed that the largest lifetime extension would be obtained by changing the fuel-element container material from stainless steel to Zircaloy.

One-dimensional radial and one-dimensional axial "window-shade" burnup calculations were compared, and the results of the two methods were in excellent agreement with regard to the predicted core lifetime. Although the radial burnup calculation is much simplier, the window-shade calculation provides essential information on axial power distribution and control-rod bank movements.

LIFETIME STUDIES FOR THE N.S. SAVANNAH REACTOR

E. E. Gross B. W. Colston
M. L. Winton

1. INTRODUCTION

In a previous study[1] Zircaloy and stainless steel were compared as fuel-element container (or egg-crate) materials in the N.S. SAVANNAH core I design. From the comparison study it was estimated that, relative to the present stainless steel fuel-element containers, a Zircaloy fuel-element container structure would increase core I control-rod worth by $\Delta k = 0.043$ and would increase core reactivity by $\Delta k = 0.062$ for the same fuel enrichment. Consequently substitution of Zircaloy for stainless steel in the N.S. SAVANNAH egg crate would allow the fuel enrichment to be reduced from 4.2 wt % U^{235} to 3.4 wt % U^{235} while maintaining the same reactivity lifetime; or, by taking full advantage of the increase in rod worth, this substitution could be used to achieve an increase in core reactivity lifetime of about 60%. Economic analysis[2] has revealed that, from a fuel-cycle cost viewpoint, a favorable way to take advantage of the properties of a Zircaloy fuel-element container assembly is to extend reactivity lifetime.

The incentive for long core life revealed by economic studies led to the burnup studies discussed in this report. These studies are limited to the core I fuel-element design,[3] with either stainless steel or Zircaloy fuel element containers. Since the prior nuclear analyses[1] for these cores provide the basis and starting point for the burnup studies, only a brief resume of the beginning-of-life core analysis is presented here. The analysis methods used in the burnup calculations are, however, discussed in more detail. These methods are then used to compare the burnup of single-zone and two-zone loadings in core I. This is followed by an investigation of various fuel-reshuffling schemes after a two-zone core I has burned up. Finally, one-dimensional radial burnup results are compared with one-dimensional axial burnup calculations using the "window-shade" method. This comparison is made for both stainless steel and Zircaloy fuel-element container cores.

2. DESCRIPTION OF THE CORE

The N.S. SAVANNAH core I design is fully described in other publications,[3] and only a brief description is provided here. A view of the top of the core is shown in Fig. 1. This reactor is a heterogeneous water-moderated and water-reflected system consisting of 32 fuel elements on a square array defined by an egg-crate-like structure presently made of stainless steel. The egg crate defines flow passages for the fuel elements and

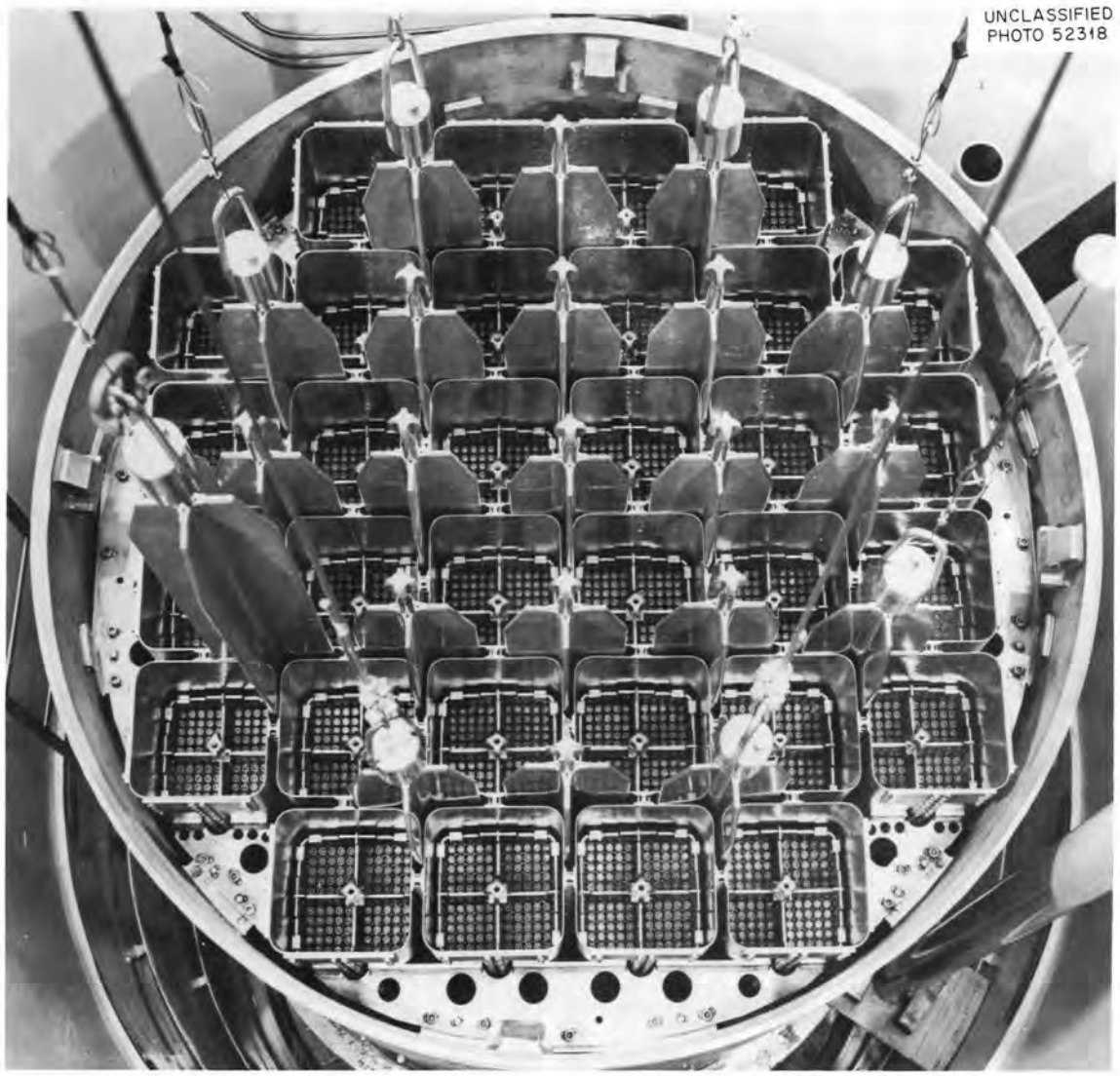

Fig. 1. Top View of N.S. SAVANNAH Core I.

provides channels for the 21 cruciform control rods and control-rod followers. A cut-away view of the egg-crate structure, unencumbered by fuel elements or control rods, is shown in Fig. 2. This entire structure can be removed as a unit. A view of one of the 6-ft active-length fuel elements that fits into the egg crate is shown in Fig. 3. A fuel element consists of 164 cylindrical stainless steel fuel tubes containing UO_2 pellets. The tubes are held in a rigid bundle by brazed stainless steel ferrules

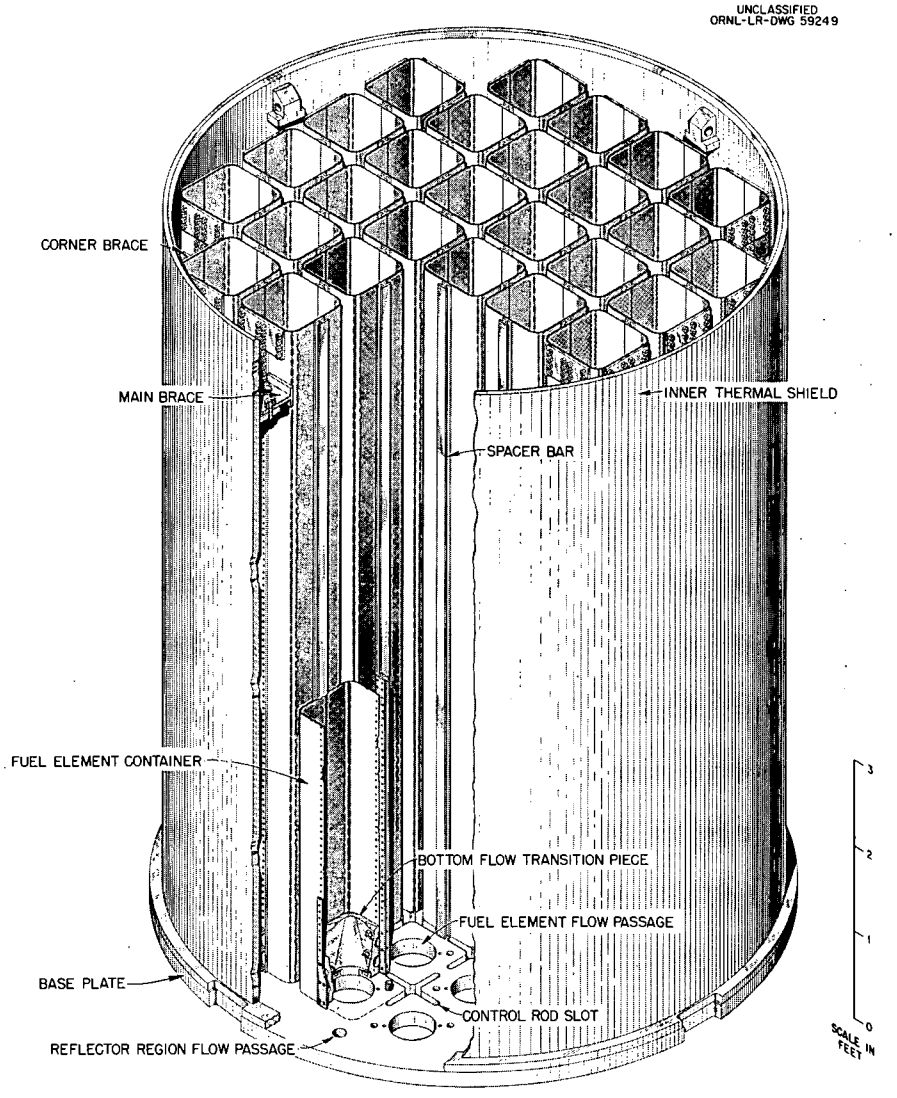

Fig. 2. N.S. SAVANNAH Fuel Element Container Assembly.

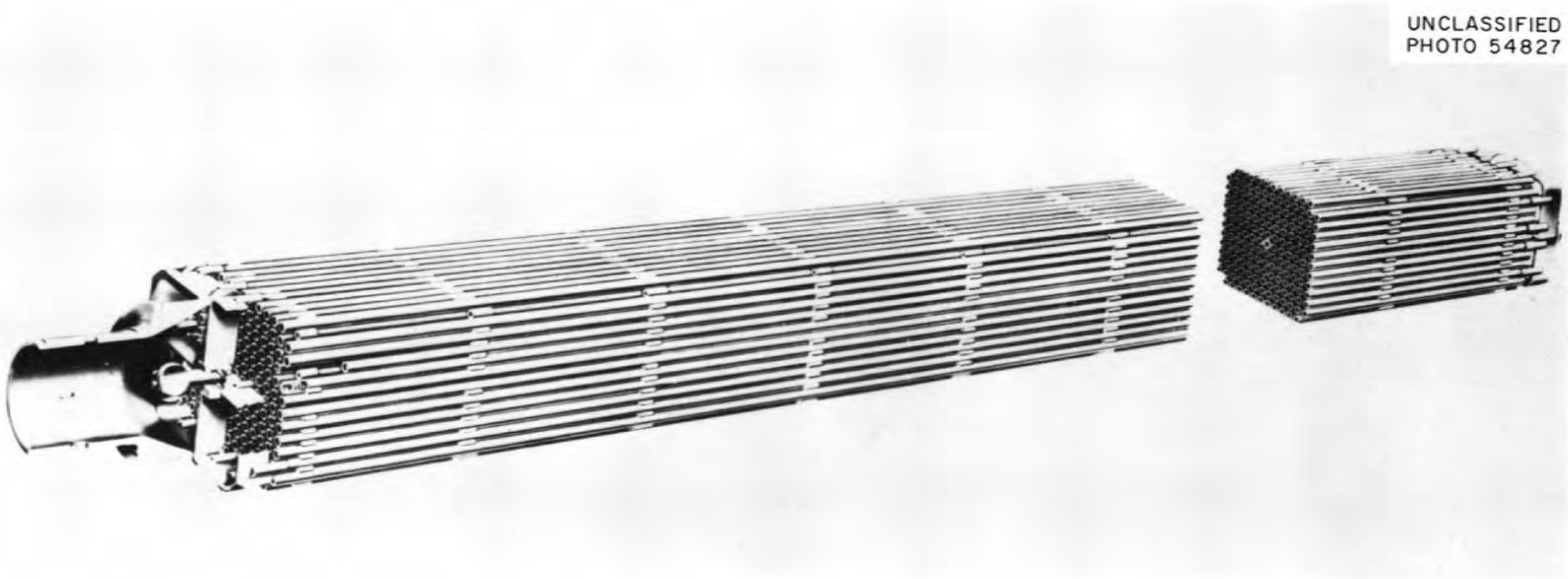

Fig. 3. N.S. SAVANNAH Core I Fuel Element.

1 in. long and located every 8 in. axially along the fuel element. Details of a section of the core through a ferrule plane are shown in Fig. 4. The design is quite complex geometrically, and many different materials are used.

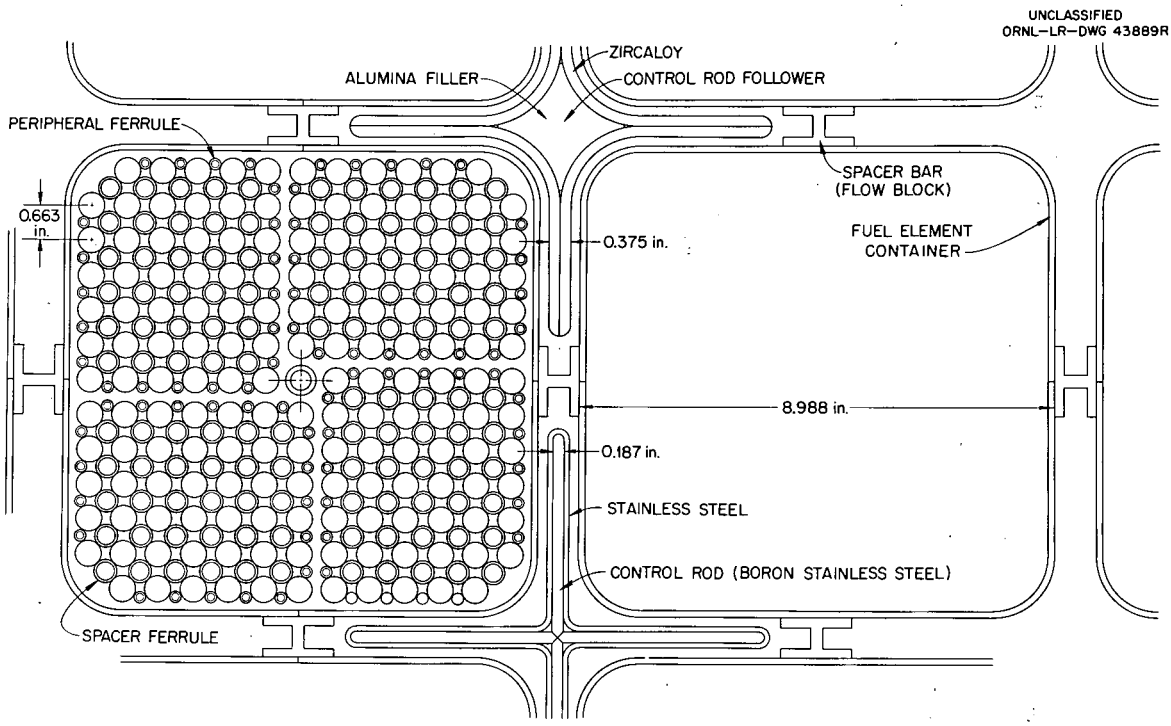

Fig. 4. N.S. SAVANNAH Core I Details. Section through a ferrule plane.

3. BEGINNING-OF-LIFE CORE ANALYSIS

A desire to study at least the two-dimensional aspects of the N.S. SAVANNAH core I design led to a four-energy-group method, since the available two-dimensional codes had a four-energy-group limit.[4] The thermal-energy-group cross sections were obtained by averaging available cross-section data over a Maxwell-Boltzmann distribution for the thermal-flux energy dependence. Deviation from a Maxwellian shape was allowed for by characterizing the Maxwellian flux distribution by a neutron temperature somewhat higher than the water-moderator temperature. This hardened temperature was obtained from the thermalization studies of Brown,[5] and the

dependence of the average thermal cross sections on moderator temperature was based on the work of Petrie, Storm, and Zweifel.[6]

A multigroup slowing-down calculation with the GNU code[7] was used to obtain flux-averaged cross sections over the three nonthermal groups. A typical slowing-down flux-lethargy distribution showing the limits of the three nonthermal groups is shown in Fig. 5. In the slowing-down calculation, the core was assumed to be homogeneous with respect to the nonthermal neutrons. The heterogeneous effect of resonance absorption in U^{238} was accounted for by generating multigroup U^{238} absorption cross sections that were consistent with a Dancoff-corrected[8] resonance integral[9] appropriate to the N.S. SAVANNAH core geometry. Other important physical effects accounted for in the determination of the slowing-down flux-lethargy dependence (Fig. 5) were (1) Goertzel-Selengut hydrogen slowing down, (2) inelastic-scattering slowing down, (3) leakage from the core, (4) absorption

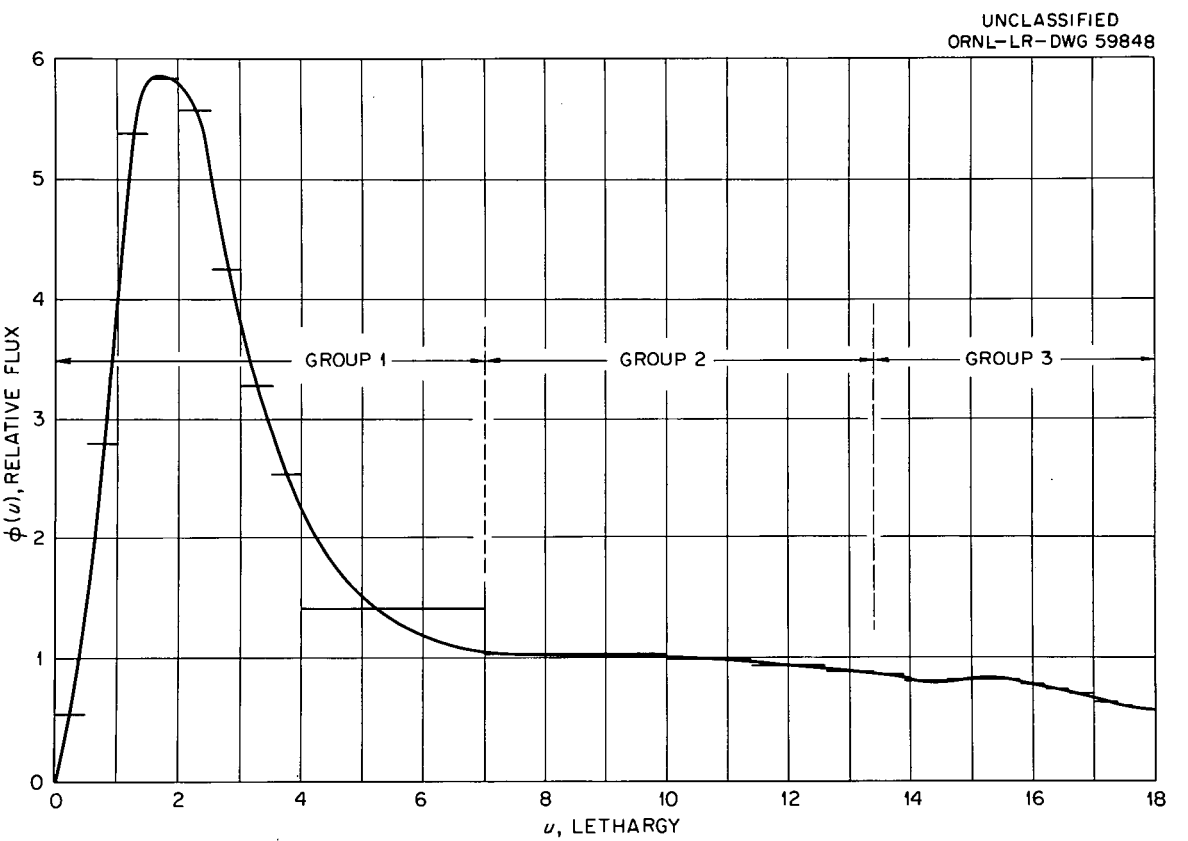

Fig. 5. Lethargy Distribution of Slowing Down Flux for Core I at 68°F.

of neutrons in all materials on the basis of available resonance integrals,[10] and (5) nonthermal fissions in U^{235} consistent with differential cross-section data[11] and consistent with the measured fission resonance integral.[10]

The four-group cross sections were then used to determine flux distributions and reaction rates throughout the reactor. This was accomplished by successive homogenization steps relying upon the symmetry properties of the core. The culmination of this process was the determination of gross flux distributions over the whole core based on the geometry of Fig. 6.

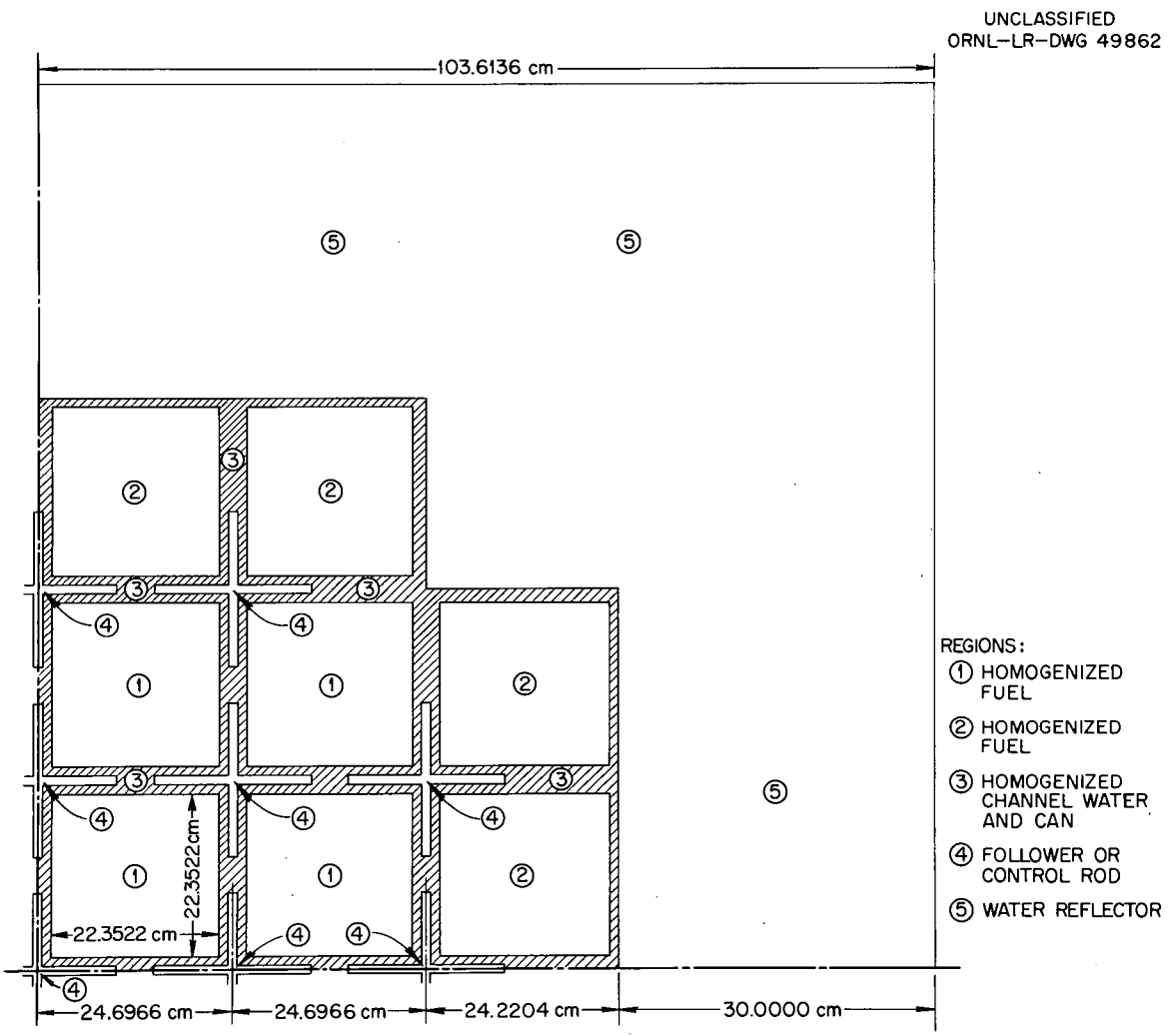

Fig. 6. Geometrical Model for One Quandrant of N.S. SAVANNAH Core I.

Calculations in the geometry of Fig. 6 employed diffusion theory,[4] with the control rods replaced by a current-per-unit-flux boundary condition at the rod surface.[12] The control-rod boundary conditions were determined by a slab geometry control-rod cell calculation using the S-5 approximation to the S_n method.[13] The S_n transport theory was also employed in the calculations of the fluxes in the strongly absorbing UO_2 region. A full account of the analysis methods was presented previously.[1]

The detail contained in the analysis method is illustrated in Fig. 7, which shows the four-group flux levels in the various core regions. The fluxes have been normalized to unity in the UO_2 fuel region in Fig. 7. Strong variation of the fast flux (group 1), as well as the thermal flux (group 4), justifies the detail put into the analysis. Knowledge of the

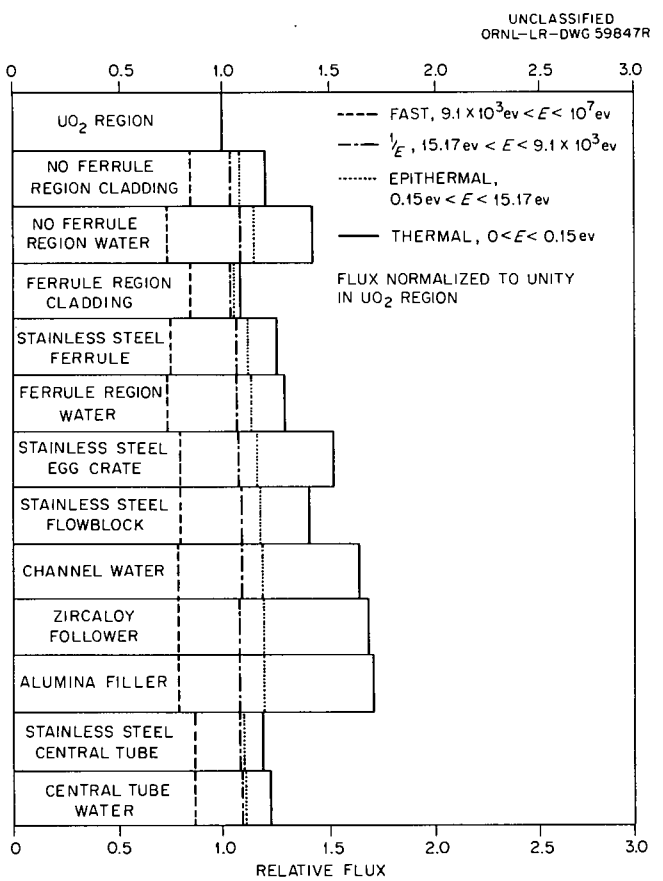

Fig. 7. Relative Four Group Fluxes in N.S. SAVANNAH Core I Components at 508°F.

four-group flux variations, as illustrated in Fig. 7, allows the determination of flux-averaged microscopic cross sections for each element in the core, which can then form the basis for a burnup calculation.

4. BURNUP ANALYSIS

Analytical Model

Burnup calculations were performed with the aid of the CANDLE code,[14] which is a one-dimensional, few-group, diffusion-theory code incorporating isotope equations. As used here, the code solves the following coupled four-group equations (with appropriate boundary conditions) for the four-group fluxes:

$$-\nabla \cdot \frac{1}{3\Sigma_{tr1}(\underline{r},t)} \nabla \phi_1(\underline{r},t) + \left[\Sigma_{a1}(\underline{r},t) + \Sigma_{12}(\underline{r},t) + \frac{B_{\perp 1}^2(\underline{r})}{3\Sigma_{tr1}(\underline{r},t)}\right] \phi_1(\underline{r},t)$$

$$= \frac{\upsilon}{k(t)} \left[\Sigma_{f1}(\underline{r},t)\, \phi_1(\underline{r},t) + \Sigma_{f2}(\underline{r},t)\, \phi_2(\underline{r},t) + \Sigma_{f3}(\underline{r},t)\, \phi_3(\underline{r},t) + \right.$$

$$\left. + \Sigma_{f4}(\underline{r},t)\, \phi_4(\underline{r},t)\right] , \quad (1a)$$

$$-\nabla \cdot \frac{1}{3\Sigma_{tr2}(\underline{r},t)} \nabla \phi_2(\underline{r},t) + \left[\Sigma_{a2}(\underline{r},t) + \Sigma_{23}(\underline{r},t) + \frac{B_{\perp 2}^2(\underline{r})}{3\Sigma_{tr2}(\underline{r},t)}\right] \phi_2(\underline{r},t)$$

$$= \Sigma_{12}(\underline{r},t)\, \phi_1(\underline{r},t) , \quad (1b)$$

$$-\nabla \cdot \frac{1}{3\Sigma_{tr3}(\underline{r},t)} \nabla \phi_3(\underline{r},t) + \left[\Sigma_{a3}(\underline{r},t) + \Sigma_{34}(\underline{r},t) + \frac{B_{\perp 3}^2(\underline{r})}{3\Sigma_{tr3}(\underline{r},t)}\right] \phi_3(\underline{r},t)$$

$$= \Sigma_{23}(\underline{r},t)\, \phi_2(\underline{r},t) , \quad (1c)$$

$$-\underline{\nabla}\cdot\frac{1}{3\Sigma_{tr4}(\underline{r},t)}\underline{\nabla}\phi_4(\underline{r},t)+\left[\Sigma_{a4}(\underline{r},t)+\frac{B^2_{\perp 4}(\underline{r})}{3\Sigma_{tr4}(\underline{r},t)}\right]\phi_4(\underline{r},t)$$

$$=\Sigma_{34}(\underline{r},t)\,\phi_3(\underline{r},t)\ , \qquad (1d)$$

where Σ_{ag} is the macroscopic absorption cross section in group g (that is, group 1, 2, 3, or 4); Σ_{trg} is the macroscopic transport scattering cross section in group g; Σ_{fg} is the macroscopic fission cross section in group g; $\Sigma_{gg'}$ is the macroscopic cross section for transfer from group g to group g′; $B^2_{\perp g}$ is the transverse buckling in group g; and k is the static multiplication factor or eigenvalue.

The macroscopic cross sections are related to the microscopic cross section by:

$$\Sigma_{ig}(\underline{r},t)=\sum_m N^m(\underline{r},t)\ \sigma^m_{ig}\ , \qquad (2)$$

where σ^m_{ig} is the type i microscopic cross section for material m in group g and $N^m(\underline{r},t)$ is the atom density of material m at time t and at position $\underline{r}$ in the reactor. It is to be noted that the microscopic cross sections are assumed to be space and time independent.

Isotope equations for the $N^m(\underline{r},t)$ are of the general form:

$$\frac{dN^m(\underline{r},t)}{dt}=\lambda^{m-1}\,N^{m-1}(\underline{r},t)-\lambda^m\,N^m(\underline{r},t)-N^m(\underline{r},t)\sum_{g=1}^{g=4}\sigma^m_{ag}\,\phi_g(\underline{r},t)\ , \qquad (3)$$

where λ^{m-1} is the decay constant of the isotope which decays into isotope m, and λ^m is the decay constant of isotope m. Isotope equations are available for U^{235}, U^{238}, Pu^{239}, Pu^{240}, Pu^{241}, Xe, Sm, and lumped fission-product poisons.

As input, CANDLE requires a one-dimensional geometry with a space mesh and boundary conditions, initial atom densities in each region, microscopic cross sections for each material, a time mesh, transverse bucklings, and a power level. Equations 1 are then solved by finite difference methods for the fluxes, ϕ, and the multiplication factor, k. With these initial fluxes,

Eq. 3 is then solved by a finite-difference approximation for the atom densities at the end of the first time interval. The new atom densities may then be inserted into Eqs. 1 and the whole process repeated. An important option allows the burnup calculation to proceed with the eigenvalue k = 1 at all times by the adjustment of a boundary position, designated the control boundary. This allows simulation of control by a control-rod bank and is sometimes referred to as the window-shade model. Another important option, the xenon-override option, can be used to determine the reactivity worth of peak xenon.

Geometry and Initial Conditions

Radial Burnup

For the radial burnup calculation the core geometry of Fig. 6 was approximated by a fuel region with a radius that gave the area of the 32 fuel elements and an annular reflector region, as shown in Fig. 8. The core was subdivided into six regions and the reflector into three regions. The inner three core regions correspond in area to the inner 16 fuel elements of 4.2-wt % enrichment. Likewise, the outer three core regions correspond in area to the outer 16 elements of 4.6-wt % enrichment. This division of areas was made to allow a simulated fuel reshuffle.

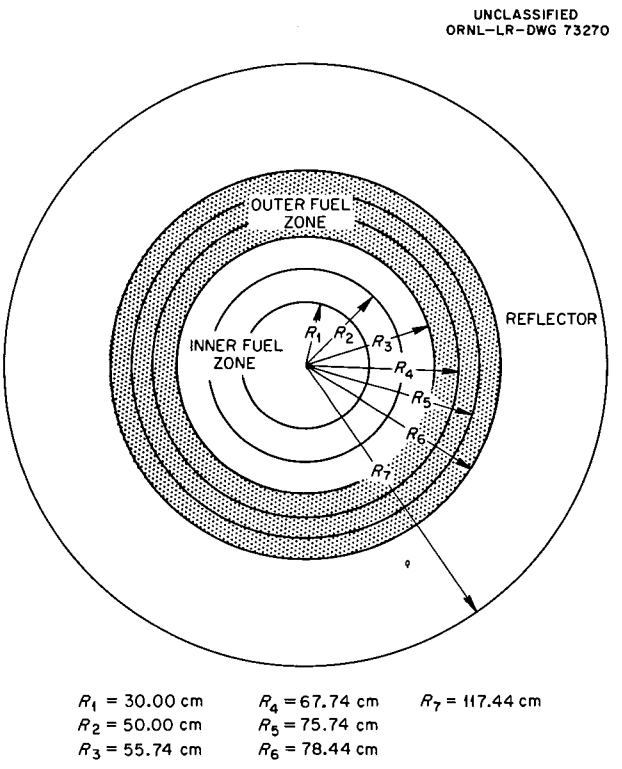

Fig. 8. Geometry Used in Radial Burnup Calculations.

Volume-averaged atom densities of 0.000236×10^{24} for U^{235} and 0.00531×10^{24} for U^{238} were used for the inner three core regions (4.2-wt % enrichment). These same

values were also used in the outer three core regions when uniform loadings were considered. For an outer fuel zone loading of 4.6 wt % U^{235}, atom densities of 0.0002548×10^{24} for U^{235} and 0.005293×10^{24} for U^{238} were used in the outer three core regions. The only other material present in the core at the beginning of life was material E. This is a fictitious element containing the information about all the structural material, channel water, followers, and control rods. For radial burnup calculations material E did not contain control-rod properties, and the core was assumed to be controlled by a uniformly distributed poison. The composition of material E does not change with time, and the atom density for this material was arbitrarily chosen to be 1×10^{24}. The atom density for the water in the reflector was taken to be 0.02601×10^{24}. All the atom densities were based on the operating temperatures of the reactor, that is, 508°F moderator and 910°F fuel temperature. Other conditions necessary for the radial burnup calculations were as follows:

Power level	63.0×10^6
Core height	167.64 cm
Axial buckling	$0.000294\ cm^{-2}$ for all regions
Time steps	First 12 time steps, $\Delta t = 1.44 \times 10^4$ sec; remaining, $\Delta t = 3.945 \times 10^6$ sec
Xenon	Reduce flux to zero and check xenon override at $\Delta t = 1.08 \times 10^4$ sec

Axial Burnup

For purposes of rod programming, the 21 control rods were grouped into units of four rods each, with the exception of the central rod, as shown in Fig. 9. An investigation[15] of two-dimensional power distributions to be expected for various control-rod patterns revealed that the most favorable power distributions occurred when the central rods (X, A, and B rods) were in the core. On this basis, an attempt was made to simulate a burnup history in which the core was initially controlled by the B-rod bank, the A rods and the X rod were fully inserted, and the outer rods (C, D, and E) were fully withdrawn. When the B rods were withdrawn as far as possible, the A-rod bank became the controlling rod bank. Total

UNCLASSIFIED
ORNL-LR-DWG 73271

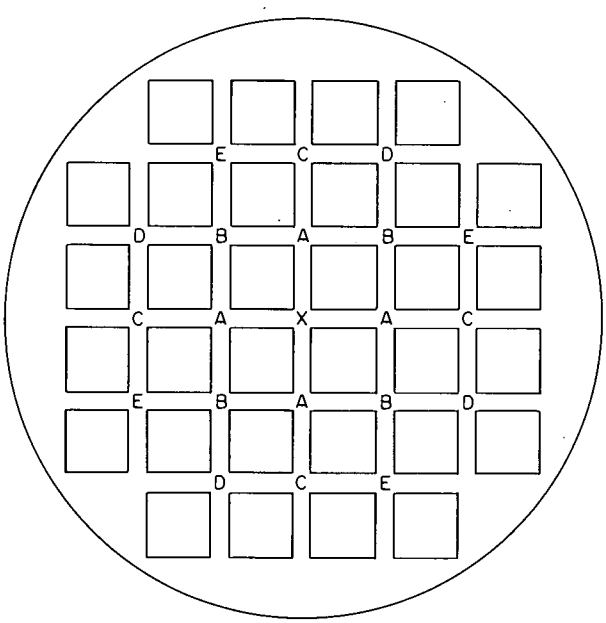

Fig. 9. N.S. SAVANNAH Rod Groups.

withdrawal of the A-rod bank was then followed by X-rod control of the reactor.

This attempt at simulating rod programming is reflected in the axial slab geometry shown in Fig. 10. Regions 3 and 7 are required because the 58-in. control-rod section is centered in the 66-in. active fuel section when fully inserted into the core; thus, there are 4-in. sections at the top and bottom of the active core region containing either all rods or all followers. The bottom boundaries of the X rod and A rods are separated for ease of transferring rod-bank control from the A rods to the X rod. Other regions in Fig. 10 are self-explanatory.

For the core I analysis the atom densities for the fuel were obtained by volume averaging the 4.2-wt % and 4.6-wt % enrichment zones. This gave an atom density of 0.000247×10^{24} for U^{235} and 0.0053×10^{24} for U^{238}. For the analysis of the Zircaloy egg-crate core all the fuel was assumed to be 4.2-wt % enriched, and the atom densities were 0.000236×10^{24} for U^{235} and 0.00531×10^{24} for U^{238}. The conditions for the axial-burnup calculations are given below and other necessary information is presented in Tables 1 and 2.

Core radius	78.44 cm
Time steps	First 12 time steps, $\Delta t = 1.44 \times 10^4$ sec; remaining time steps, $\Delta t = 3.945 \times 10^4$ sec

It should be noted that in the axial burnup, k_{eff} is kept equal to 1.0 by adjustment of a boundary between the poisoned and unpoisoned portion of the core, and the calculation stops when the upper limit for the specified control boundary is reached. This necessitates doing the calculation in steps, by first allowing the initial boundary to come out to

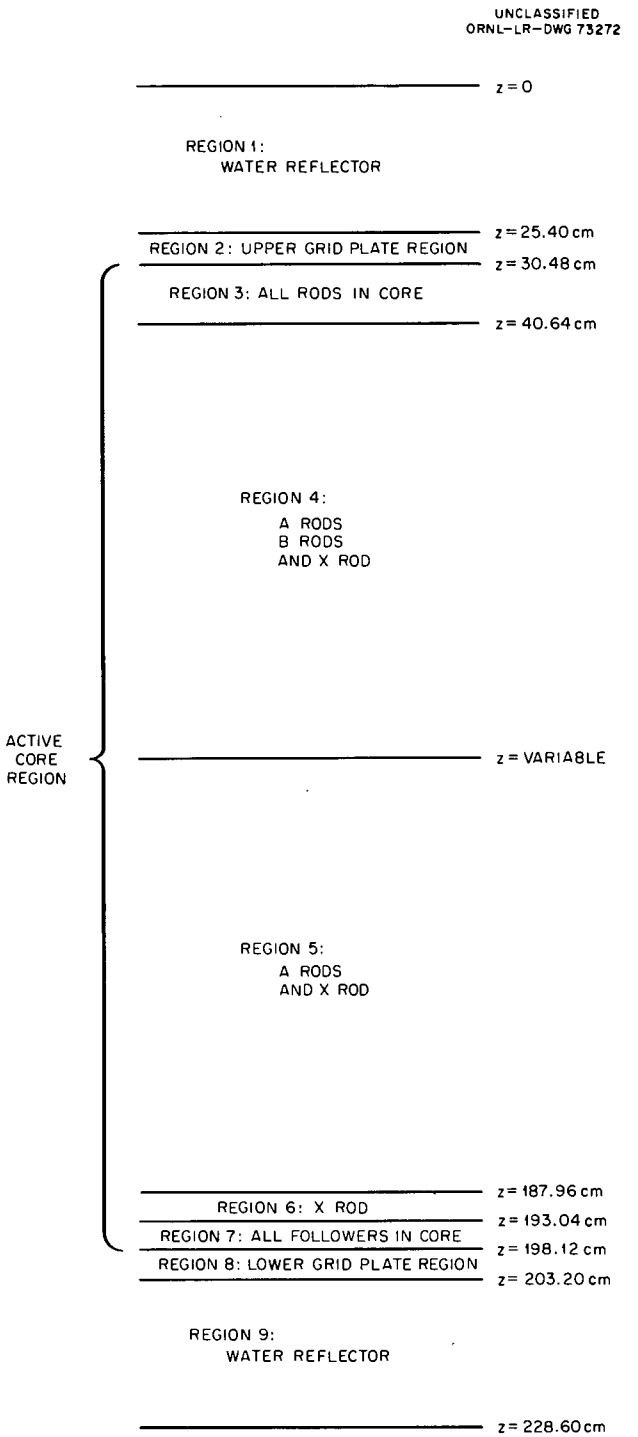

Fig. 10. Axial Geometry Used in Window-Shade Burnup Calculations.

Table 1. Radial Buckling Data for Core I with Stainless Steel Egg Crate

Region	Radial Buckling (cm^{-2})			
	Group 1	Group 2	Group 3	Group 4
1, 2, 3	0.002503	0.0011047	0.000386	-0.03182682
4	0.002441	0.0010163	0.000291	-0.023824
5	0.0019931	0.0008314	0.00248	-0.0187461
6	0.00150287	0.0006286	0.000198	-0.013491
7, 8, 9	0.001332	0.0005578	0.000179	-0.011769

Table 2. Radial Buckling Data for 4.2-wt % Enriched Zircaloy Egg-Crate Core

Region	Radial Buckling (cm^{-2})			
	Group 1	Group 2	Group 3	Group 4
1, 2, 3	0.002897	0.001443	0.000981	-0.02710
4	0.002755	0.001126	0.000437	-0.01891
5	0.002217	0.000914	0.000366	-0.01495
6	0.001629	0.000678	0.000284	-0.010693
7, 8, 9	0.0014212	0.000594	0.0002522	-0.00923

a maximum value and then continuing the calculation by specifying a new boundary. None of the calculated information is lost by this procedure.

Cross Sections and Bucklings

Flux-averaged microscopic cross sections for U^{235} and U^{238} were obtained from the detailed core analysis.[1] The other core materials, which do not burn up, were lumped together as a single material, designated by the superscript E, and were assigned flux-averaged cross sections appropriate to reaction rates computed in the beginning-of-life core analysis. Plutonium isotopes and fission products, since they are formed in the UO_2 fuel region, were assigned cross sections weighted by the average fluxes

in the fuel region. All microscopic cross sections were assumed to be time independent, which amounts to assuming that the average fluxes in each core region (Fig. 7) do not change with burnup.

As mentioned, the control rods were treated by transport-theory equivalent boundary conditions for the ratio of the current to the flux at the control-rod surface. That is, constants C_g were specified at the control-rod surface to give

$$-C_g = \left[\frac{\underline{n} \cdot \underline{J}_g(\underline{r})}{\phi_g(\underline{r})}\right]_S , \tag{4}$$

where $\underline{n}$ is a unit vector normal to the control-rod surface S and $\underline{J}_g(\underline{r})$ is the neutron current density in group g at position $\underline{r}$. Within the control rod the following balance equation holds:

$$\underline{\nabla} \cdot \underline{J}_g(\underline{r}) = -\Sigma_{ag}^{rod} \phi_g(\underline{r}) , \tag{5}$$

where Σ_{ag}^{rod} is the macroscopic absorption cross section of the control rod in the group g. By integrating Eq. 5 over the volume of the rod and using Green's theorem, it is shown that

$$\oint_S \underline{n} \cdot \underline{J}_g(\underline{r}) \, ds = -\Sigma_{ag}^{rod} \int_V \phi_g(\underline{r}) \, dV , \tag{6}$$

where the integral on the left is around the control-rod surface S and the integral on the right is over the control-rod volume V. Combining Eqs. 4 and 6, the control-rod absorption rate can be related to the average control-rod surface flux, $\overline{\phi}_{gS}$, by

$$\Sigma_{ag}^{rod} \int_V \phi_g(\underline{r}) \, dV = C_g A_S \overline{\phi}_{gS} , \tag{7}$$

where A_S is the control-rod surface area. The beginning-of-life core analysis provided the necessary information to calculate* $\bar{\phi}_{gS}$, as well as C_g, and the absorption rate of the control rods could then be computed from Eq. 7. In this way the effect of control-rod absorptions into material E could be lumped.

In addition to the cross sections, the transverse bucklings must also be provided for Eqs. 1. For radial burnup calculations, an axial buckling of 0.000294 cm^{-2} was used in each group. This value was obtained from axial flux profiles measured in the N.S. SAVANNAH critical experiments.[16] For window-shade burnup calculations, transverse bucklings in each group were obtained from the following balance equations:

$$\left(\overline{\frac{1}{3\Sigma_{tr1}}}\right) B_{\perp 1}^2 = \frac{\upsilon F^{xy}}{k} - A_1^{xy} - T_{12}^{xy} - L_1^z \quad , \tag{8a}$$

$$\left(\overline{\frac{1}{3\Sigma_{tr2}}}\right) B_{\perp 2}^2 = T_{12}^{xy} - A_2^{xy} - T_{23}^{xy} - L_2^z \quad , \tag{8b}$$

$$\left(\overline{\frac{1}{3\Sigma_{tr3}}}\right) B_{\perp 3}^2 = T_{23}^{xy} - A_3^{xy} - T_{34}^{xy} - L_3^z \quad , \tag{8c}$$

$$\left(\overline{\frac{1}{3\Sigma_{tr4}}}\right) B_{\perp 4}^2 = T_{34}^{xy} - A_4^{xy} - L_4^z \quad , \tag{8d}$$

where the first term is the flux-averaged diffusion coefficient in group g for the core region; F^{xy} is the total fission reaction rate in the core; A_g^{xy} is the total absorption reaction rate for the core in group g; $T_{gg'}^{xy}$ is the rate at which neutrons are transferred from group g to group g′ for the core region; and L_g^z is the total loss rate of neutrons from the core in group g by leakage. All these quantities result from PDQ calculations in the geometry of Fig. 6 for particular control-rod patterns. The resulting transverse bucklings for the rod patterns considered were listed in Tables 1 and 2.

---

*This calculation was automated with the PDQ code by J. W. Miller, Central Data Processing, K-25.

5. COMPARISON OF ONE- AND TWO-ZONE CORE REACTIVITY LIFETIMES

The initial core I loading for the N.S. SAVANNAH consists of 4.2 wt % U^{235} in the inner 16 fuel elements and 4.6 wt % U^{235} in the outer 16 fuel elements. This nonuniform fuel loading is important in any study of fuel reshuffling, but it was felt to be an unnecessary complication in the earlier work of comparing the virtues of Zircaloy and stainless steel as fuel-element container materials. The effect on reactivity lifetime of replacing the actual two-zone loading by a single-zone loading with the inner-zone enrichment was therefore investigated.

In the method used for generating flux-averaged microscopic cross sections, it is evident that two sets of microscopic cross sections are obtained: one for the inner-zone materials and one for the outer-zone materials. These values are listed in Table 3. As mentioned previously, the CANDLE code, as presently constituted, is limited to a single set of four-group cross sections for each fissionable material. The fuel was, therefore, characterized by cross sections pertinent to the inner fuel zone, since this is the most important part of the core. The effect of this approximation on reactivity lifetime should be small, since a small underestimation of cross section will produce a small overestimation of the flux, and the important product of flux and cross section should remain relatively unchanged.

With the above limitation on fuel cross sections, the reactivity lifetimes of single-zone and two-zone cores are compared in Fig. 11 for stainless steel fuel-element containers. The initial sharp drop in reactivity is due to the buildup of the fission-product poison Xe^{135}. Following the buildup of equilibrium samarium (~0.3 years), the multiplication factor as a function of time appears to be remarkably linear with the slope, 0.036 Δk/year. Evidently the two-zone core increases the reactivity lifetime of the one-zone core by only about one month. A single-zone core treatment should, therefore, be suitable for many kinds of studies.

Gross radial peak-to-average power distributions at the beginning of life calculated by CANDLE for the one- and two-zone cores are shown in Fig. 12. The two-zone core has a smaller peak-to-average radial power ratio

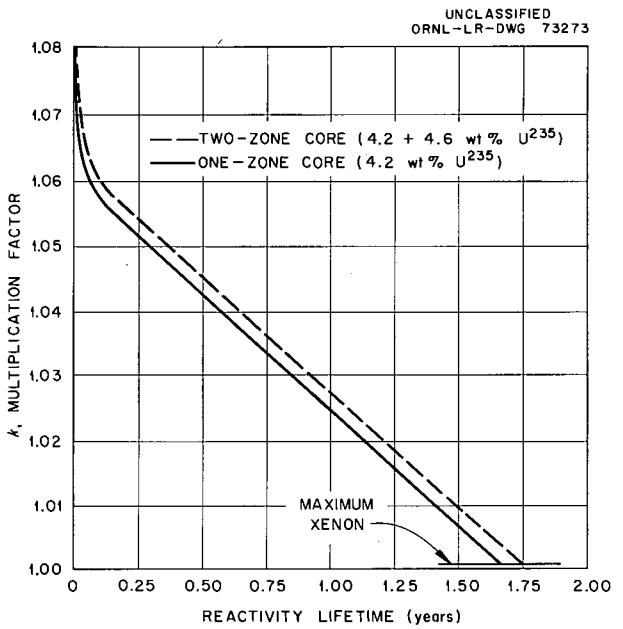

Fig. 11. Comparison of Reactivity Lifetimes of One and Two Fuel Zones in N.S. SAVANNAH Core I.

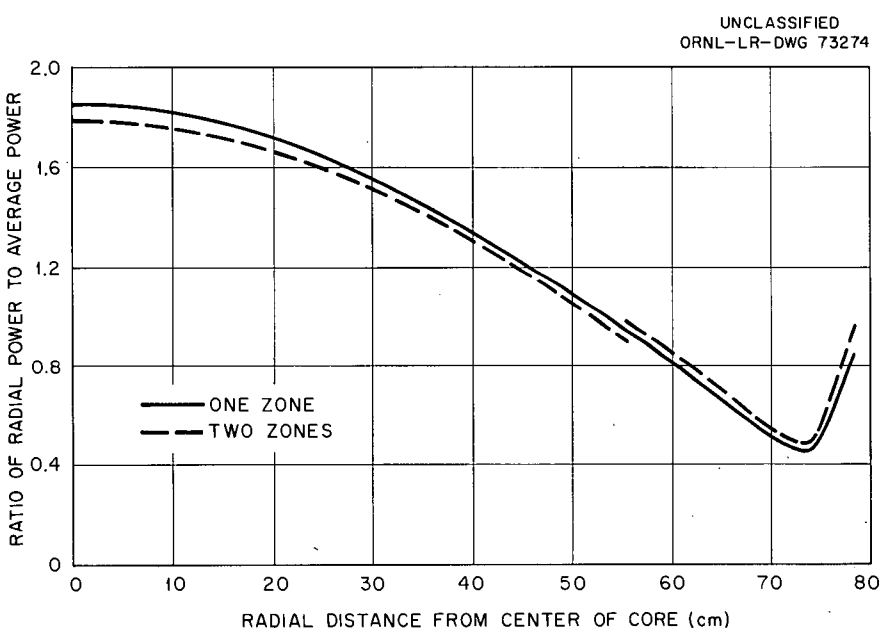

Fig. 12. Comparison of Radial Power Distributions for One and Two Fuel Zones in Core I at Beginning of Life.

Table 3. Flux-Averaged Microscopic Cross Sections for Inner and Outer Core I Fuel Zones at 508°F

Cross Section Calculated	Microscopic Cross Sections (barns)					
	U^{235}		U^{238}		E	
	Inner Zone	Outer Zone	Inner Zone	Outer Zone	Inner Zone	Outer Zone
$3\sigma_{tr1}$	31.43	31.78	20.31	20.54	0.4345	0.4340
σ_{a1}	2.59	2.62	0.479	0.485	0.0011	0.0011
σ_{12}	0	0	0.0047	0.0048	0.0285	0.0289
$\upsilon\sigma_{f1}$	5.30	5.36	0.615	0.622	0	0
$3\sigma_{tr2}$	44.38	44.63	29.48	29.64	1.1662	1.1869
σ_{a2}	29.05	29.21	1.59	1.60	0.0028	0.0027
σ_{23}	0	0	0	0	0.0806	0.0818
$\upsilon\sigma_{f2}$	44.67	44.92	0	0	0	0
$3\sigma_{tr3}$	75.71	75.65	26.80	26.78	1.2829	1.3146
σ_{a3}	87.55	87.48	1.34	1.34	0.0054	0.0057
σ_{34}	0	0	0	0	0.1174	0.1194
$\upsilon\sigma_{f3}$	154.3	154.2	0	0	0	0
$3\sigma_{tr4}$	233.2	220.7	21.33	20.19	2.4123	2.6214
σ_{a4}	326.9	309.4	1.37	1.30	0.0292	0.0333
$\upsilon\sigma_{f4}$	674.0	638.0	0	0	0	0

(P_{max}/P_{av} = 1.80) than the uniformly loaded core (P_{max}/P_{av} = 1.86). The flatter radial-power distribution of the two-zone loading is vitiated with burnup, as shown by the power distributions at the end-of-core life, presented in Fig. 13. Comparison of Figs. 12 and 13 reveals the trend toward a flatter power distribution as fuel is consumed.

Of interest to the reactor operator are the core inventories of fissionable material. These materials are also of importance in fuel-cycle economic analyses.[2] For these reasons the calculated time dependence of U^{235}, Pu^{239}, and Pu^{241} core inventories for the two-zone prototype core

are presented in Figs. 14, 15, and 16, respectively. The burnup of U^{235} is fairly linear (Fig. 14), with a slope of about 25 kg per full-power year.

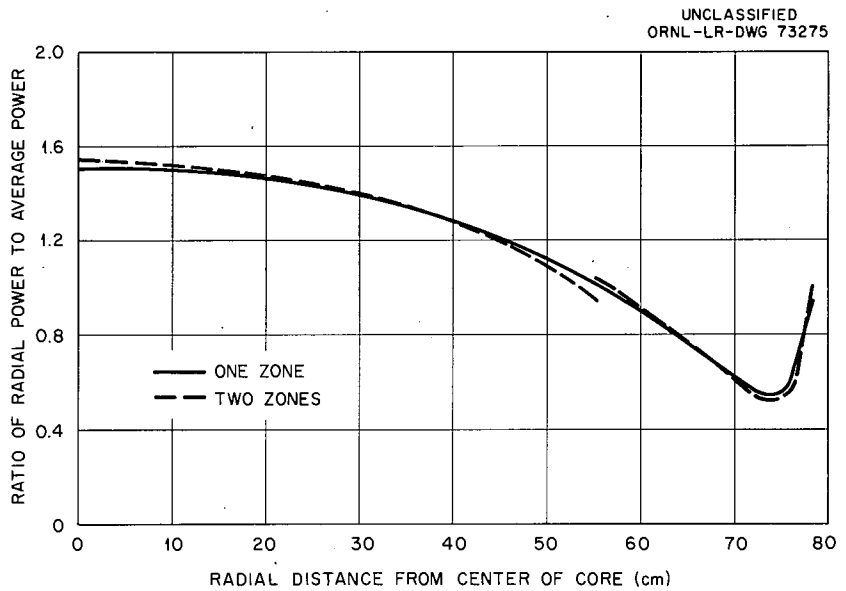

Fig. 13. Comparison of Radial Power Distributions for One and Two Fuel Zones in Core I at End of Life.

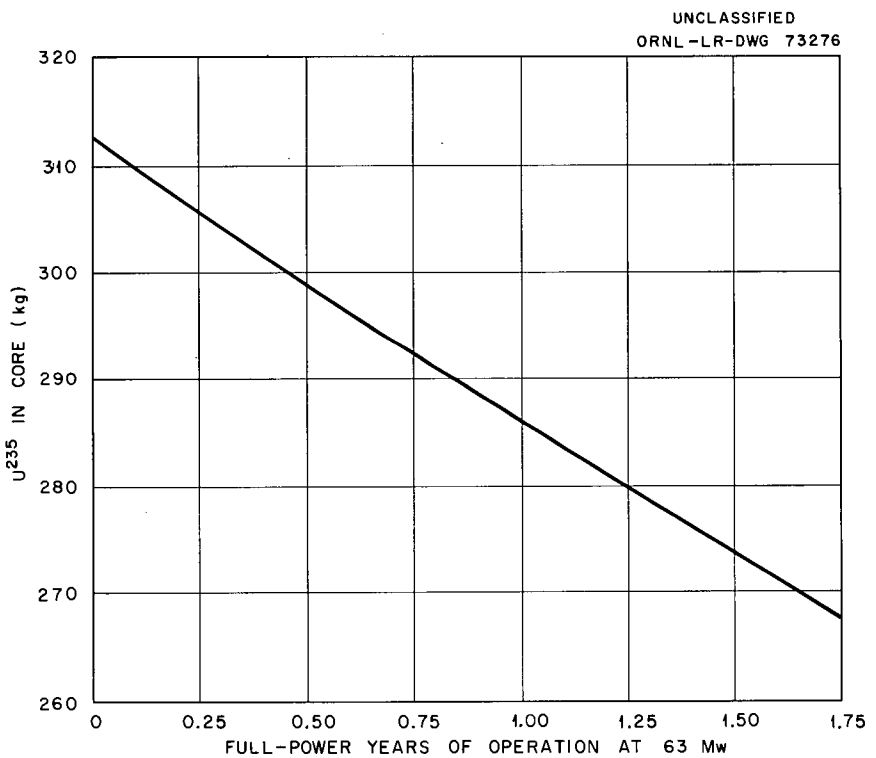

Fig. 14. Calculated Core Inventory of U^{235} in Two-Zone Core I as a Function of Full-Power Years of Operation at 63 Mw.

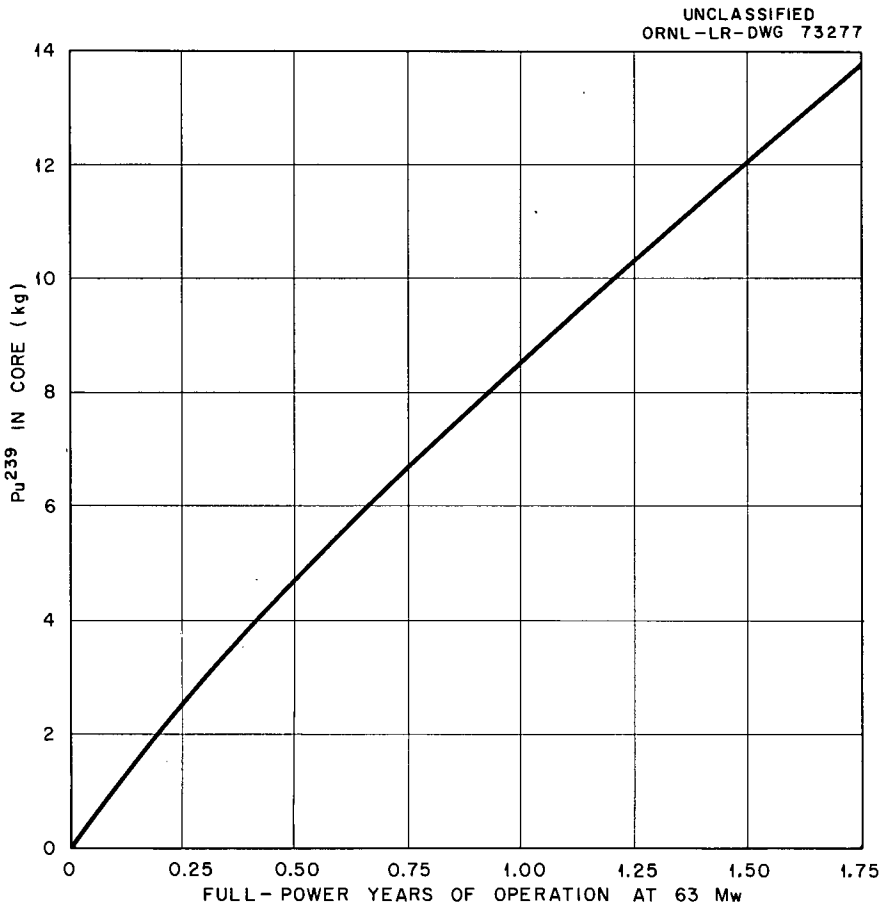

Fig. 15. Calculated Core I Inventory of Pu^{239} in Two-Zone Core I as a Function of Full-Power Years of Operation at 63 Mw.

The buildup of Pu^{239} (Fig. 15) occurs at a rate of about 8 kg per full-power year during the first full-power year and at the rate of about 6 kg per full-power year during the second year of full-power operation. The buildup of Pu^{241} is quadratic in nature, depending as it does on the build-up of intermediate isotopes of plutonium. These calculated plutonium inventories depend directly on the assumed resonance absorption integral of U^{238} (20.35 barns in this study). At the end of core life (~1.7 full-power years) the plutonium isotopes contribute about 10% of the power production, U^{238} contributes about 9%, and U^{235} provides the remainder.

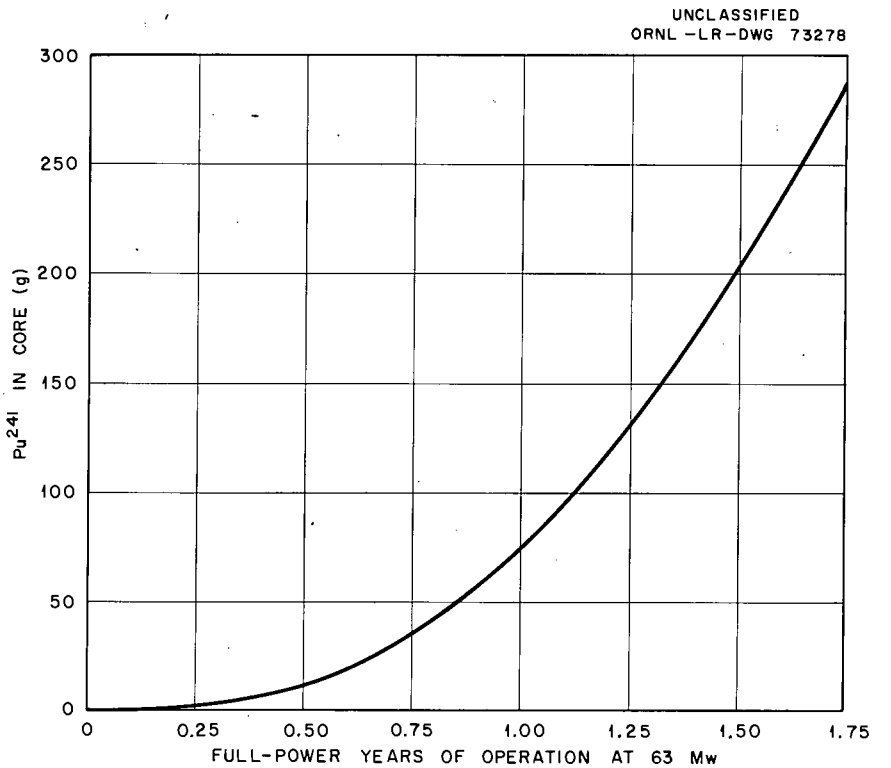

Fig. 16. Calculated Core Inventory of Pu^{241} in Two-Zone Core I as a Function of Full-Power Years of Operation at 63 Mw.

6. EFFECT OF FISSION-PRODUCT NONTHERMAL ABSORPTIONS ON REACTIVITY LIFETIME

In the burnup calculations reported here, the fission products are characterized by a single element with a thermal-absorption cross section of 43 barns at 2200 m/sec and a resonance-absorption integral of 214 barns[17] (before flux weighting). It has been customary to neglect nonthermal absorptions in fission-product poisons, mainly because of the scarcity of experimental information for these nuclei. In order to test the effect of nonthermal absorptions in fission products on the calculated lifetime of the N.S. SAVANNAH core I, an additional burnup calculation was performed using a zero resonance integral for the fission products. The calculated reactivity lifetimes for the two assumed values of the resonance-absorption integral for fission products are compared in Fig. 17. It is apparent from

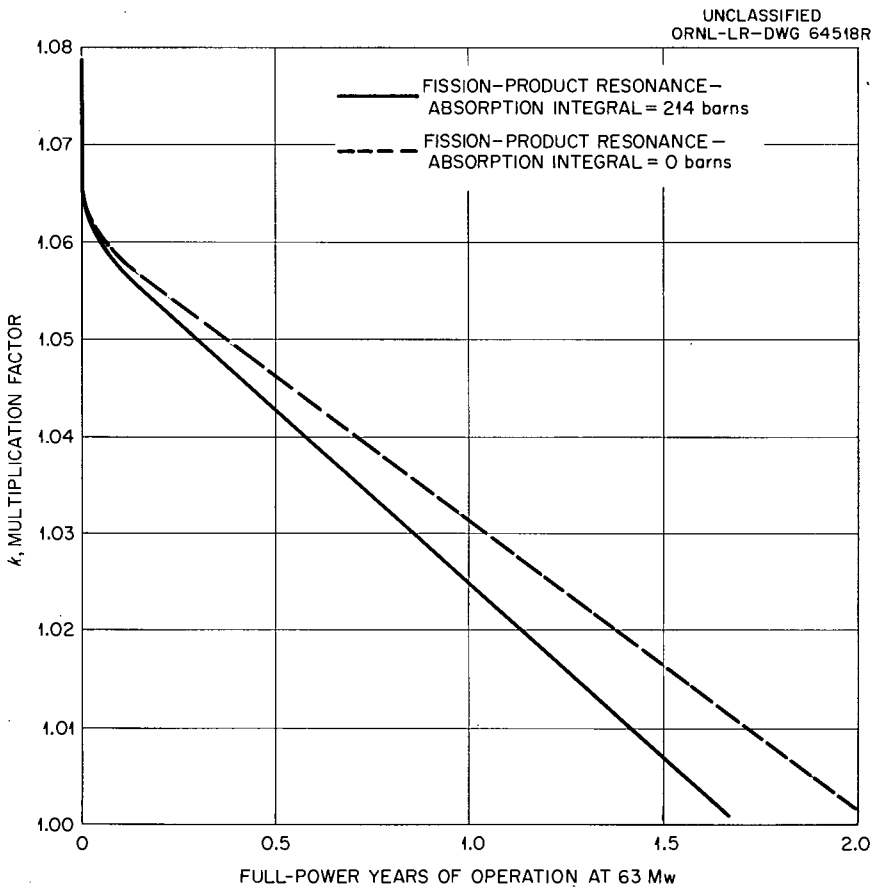

Fig. 17. Dependence of Calculated Reactivity Lifetime of N.S. SAVANNAH Core I on Resonance-Absorption Integral of Fission-Product Poisons.

this figure that calculated lifetimes for N.S. SAVANNAH-type cores are sensitive to resonance absorptions in fission products.

7. INVESTIGATION OF FUEL-RESHUFFLING SCHEMES

Additional lifetime studies were undertaken using the CANDLE code to investigate the effects of various fuel-management schemes on the burnup of an initial two-zone core I (4.2 wt % U^{235} inner zone, 4.6 wt % U^{235} outer zone). The schemes examined were (1) switching inner and outer fuel zones at the end of core I burnup; (2) removing the burned inner zone, replacing it with the burned outer zone, and inserting a fresh outer zone; and (3) leaving the burned core I fuel in place but replacing the stainless steel

egg crate with a Zircaloy egg crate. Movement of burned fuel would be accompanied by movement of the associated fission products, including equilibrium xenon and samarium.

Calculated reactivity lifetimes for these schemes are shown in Fig. 18. Of the three fuel-management schemes studied, replacement of the stainless steel egg crate by a Zircaloy egg crate (scheme 3) in a burned core I is the most attractive from the point of view of increased reactivity lifetime, since almost 3.5 full-power years of energy production are obtained from the initial fuel loading.

Simple switching of the burned zones (scheme 1) provides only an additional seven months of core life and appears to be the least attractive of the fuel-management schemes. The initial curvature in the reactivity-lifetime curve for scheme 1 is the result of the difference between the equilibrium xenon and samarium concentrations before and after the switch is made.

Addition of half a fresh core (4.6 wt % U^{235}) to the outer zone (scheme 2) is calculated to extend core life an additional 1.2 years. An enrichment of 5.65 wt % U^{235} in the fresh outer zone is required to obtain a core life equal to that obtainable from an exchange of egg-crate materials (scheme 3).

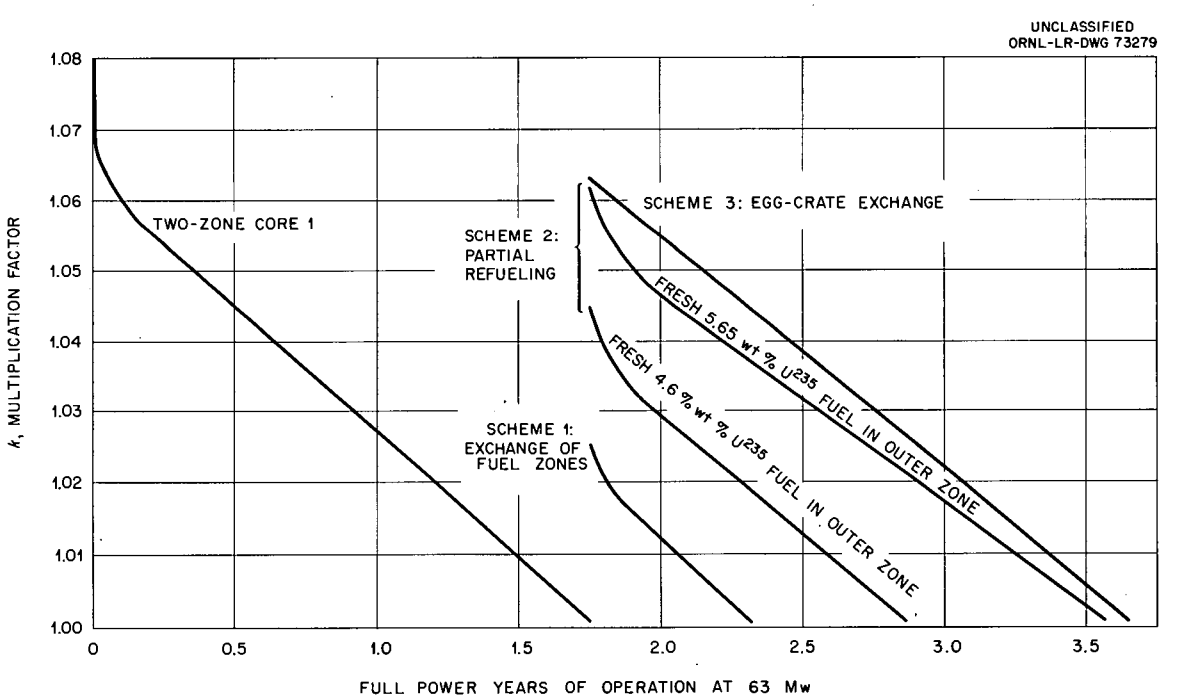

Fig. 18. Fuel-Management Studies for Two-Zone Core I.

8. COMPARISON OF AXIAL SLAB-GEOMETRY MODEL WITH EXPERIMENT

The beginning-of-life core analysis methods were compared with experimental information on core reactivity and total control-rod worth and found to be satisfactory.[1] Additional checks on the axial slab-geometry model used in the window-shade burnup calculations were desired, however. One available check was the critical A control-rod bank position measured in the zero-power experiments[18] on the prototype core. With all other control rods fully inserted, the cold, clean core was found to be critical at an A control-rod bank position of 79.0 ± 1 cm, as measured from the bottom of the active fuel region. For this same control-rod configuration, the analysis methods described here gave a multiplication factor of 1.005 at an A-bank position of 79.0 cm and k = 1.000 for an A-rod bank position of 69.5 cm.

Good agreement was also obtained for the comparison of calculated and measured control-rod axial power distributions for the critical A-bank experiment. The experiment[18] showed the power distribution to be spatially dependent; however, the calculated position for the peak power agreed with the experimental position, and the shape of the calculated axial power distribution agreed with power profiles measured near the center of the fuel elements, as may be seen in Fig. 19.

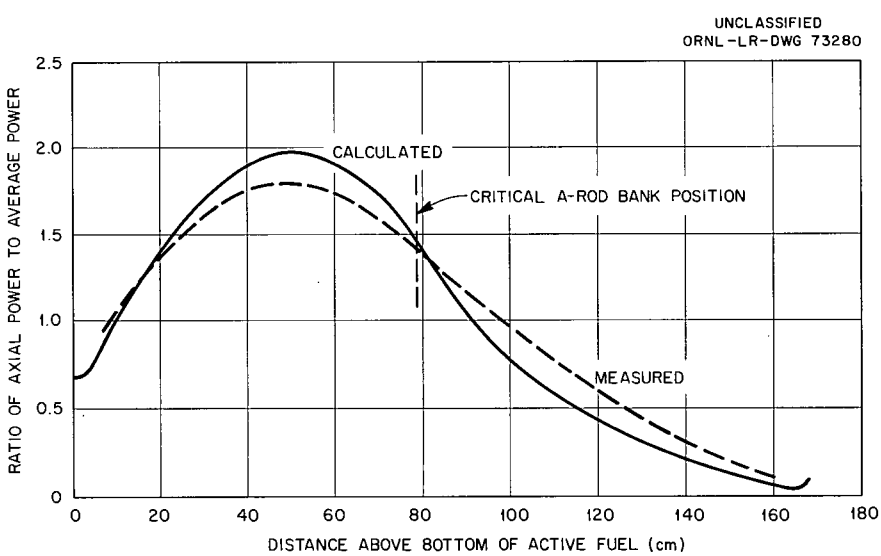

Fig. 19. Comparison of Calculated and Measured Axial Power Profiles for N.S. SAVANNAH Core I at 68°F with A-Rod Bank at 79 cm and all Other Rods Fully Inserted. Experimental curve is representative of conditions near the center of a fuel element.

9. COMPARISON OF RADIAL AND WINDOW-SHADE BURNUP METHODS FOR N.S. SAVANNAH CORE I CALCULATIONS

Radial-Burnup Lifetime Results

Comparison of reactivity lifetimes for Zircaloy and stainless steel egg-crate cores containing a uniform loading of 4.2 wt % U^{235} were reported previously[1] based on a radial burnup calculation. These calculations were for cores without control rods, control being accomplished by a uniformly distributed poison. For completeness and for contrast with the window-shade burnup calculations, these results are again presented in Fig. 20. Apparently, the use of a Zircaloy fuel-element container structure would double the reactivity lifetime of 4.2 wt % U^{235} core I fuel elements relative to their reactivity lifetime in a stainless steel fuel-element container structure.

Window-Shade-Burnup Lifetime Results

Because of the striking effect of the Zircaloy egg crate on fuel-element reactivity lifetime, it was desirable to repeat the above comparison by another, more realistic method. The one-dimensional window-shade method which allows simulation of axial rod-bank control was used. In addition

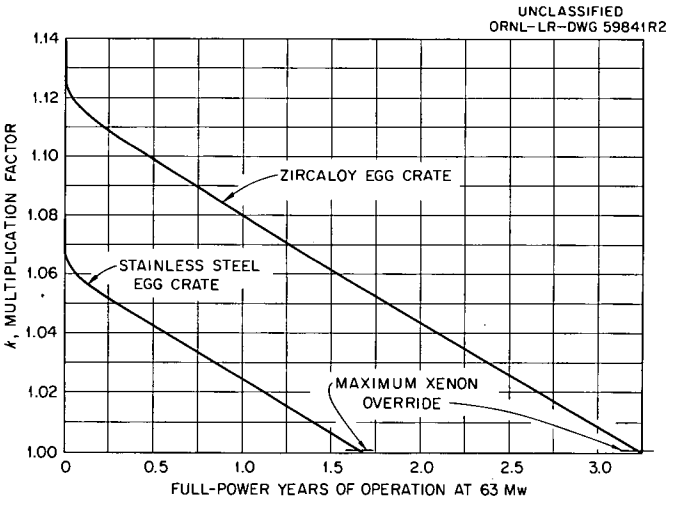

Fig. 20. Calculated Reactivity Lifetime of 4.2 wt % U^{235} Core I Fuel in Zircaloy and in Type 304 Stainless Steel Egg Crates at a Power Level of 63 Mw.

to being programmed directly in terms of an actual observable position (the controlling rod-bank position), the window-shade method provides information on the axial power distribution and on how it changes with burn-up. Since the properties for each axial zone in the window-shade calculation were obtained from two-dimensional PDQ calculations in the horizontal plane, the combination of window-shade and PDQ calculations provided some information on three-dimensional power distributions within the core.

The control-rod programming scheme simulated here was based on withdrawal of rod banks from the outer regions of the core first. For the stainless steel egg-crate core, this procedure results in a critical B-rod bank position at 24 in. withdrawn; X and A rods fully inserted; and the C, D, and E rods fully withdrawn. As the core burns up, the B-rod bank is withdrawn, followed by the A-rod bank, and then finally by the X rod. The calculated results for this mode of rod programming are presented in Fig. 21.

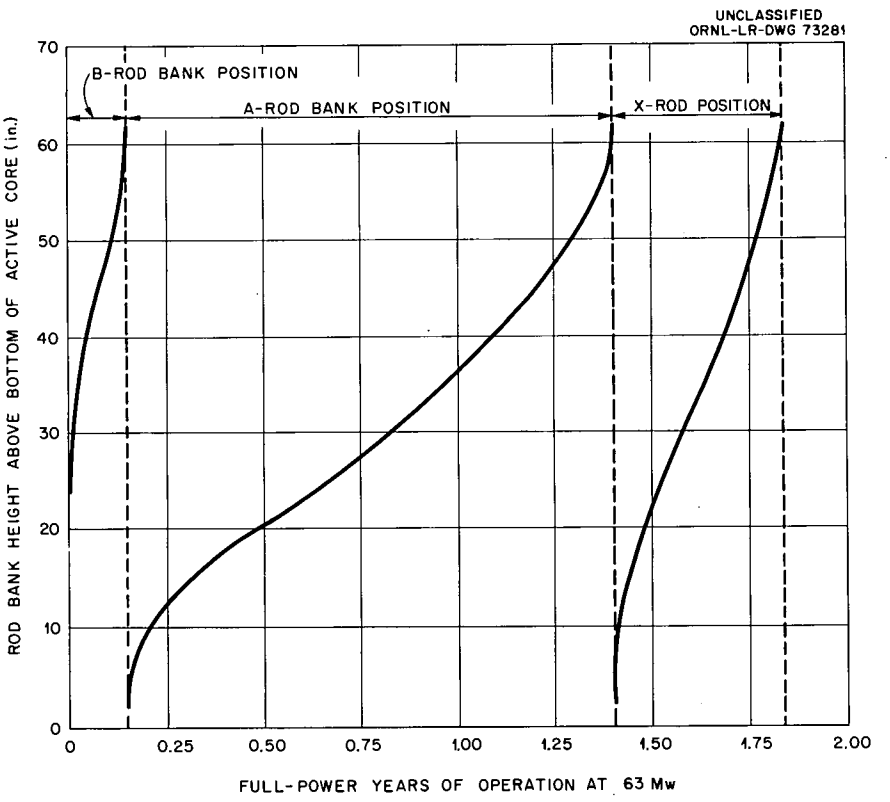

Fig. 21. Calculated Controlling Rod-Bank Position as a Function of Time for Two-Zone Core I Operating at 63 Mw.

It is to be noted that this method of burnup calculation predicts a slightly greater core life than the radial burnup calculation. This was to be expected, since the rod-programming scheme employed in the window-shade calculation produces more uniform U^{235} fuel depletion than does a radial-burnup calculation with all rods out of the core. Also the rod-bank worth is slightly asymmetrical, the rods being worth slightly more in the bottom half of the core than in the top half. This is borne out by the calculated rod-bank worths as a function of bank position shown in Fig. 22. The rod worths shown in Fig. 22 are the worths within the rod configuration experienced in the burnup calculation. For example, the B-rod bank worth curve was calculated in the geometry of Fig. 10 for the X and A rods fully inserted and the C, D, and E rods fully withdrawn. It is believed that the presence of the full-rod region at the top of the core and its absence at the bottom produces the slightly asymmetrical rod-worth curves.

The rod-worth curves may be used to convert the burnup curve of Fig. 21 into a reactivity-lifetime curve similar to that of Fig. 20. If this

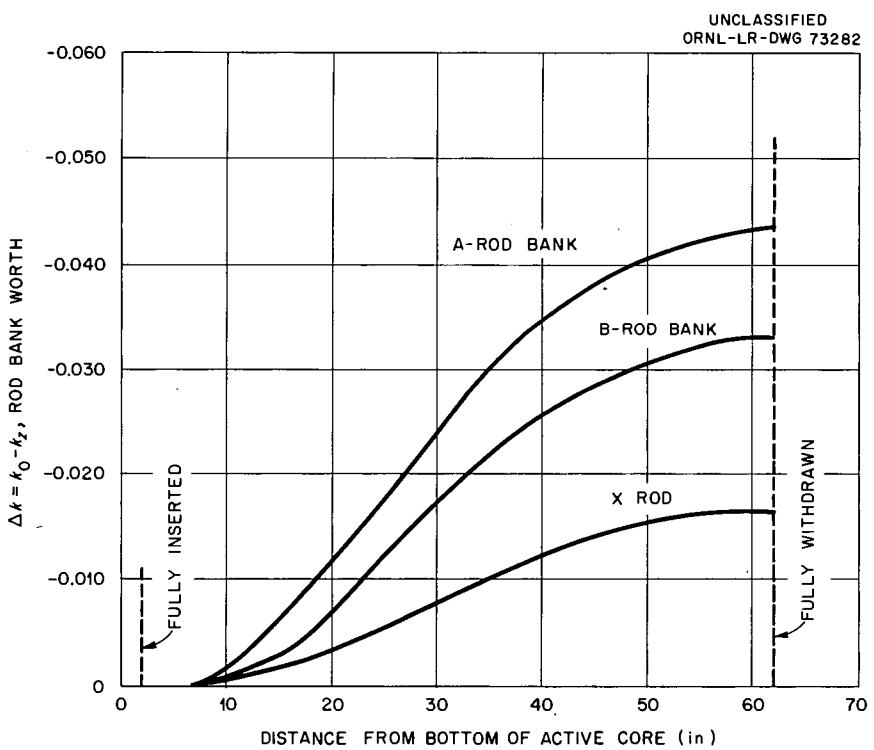

Fig. 22. Rod-Bank Worth as a Function of Bank Position Relative to Fully Inserted Position for Core I.

is done, the initial multiplication factor is found to agree with the value in Fig. 20 to within about $\Delta k = 0.002$. The window-shade burnup results are presented in the form of Fig. 21 to properly contrast the results of this method with the results of the radial-burnup calculations.

Axial Power Distributions

Axial power distributions at the beginning and end of the N.S. SAVANNAH core I life obtained from the window-shade burnup calculations are shown in Fig. 23. Examination of the burnup results at intermediate time steps reveals that the axial power distribution of the beginning of core life is the most severe with respect to the axial peak-to-average power ratio; however, this axial peak occurs in the region of the core containing A and X rods which have a favorable radial power distribution. Radial power peaking values at the beginning of core I life for various rod patterns are listed in Table 4 and were obtained from PDQ calculations in the x-y geometry of Fig. 6. Combining radial and axial peaking factors, it is apparent

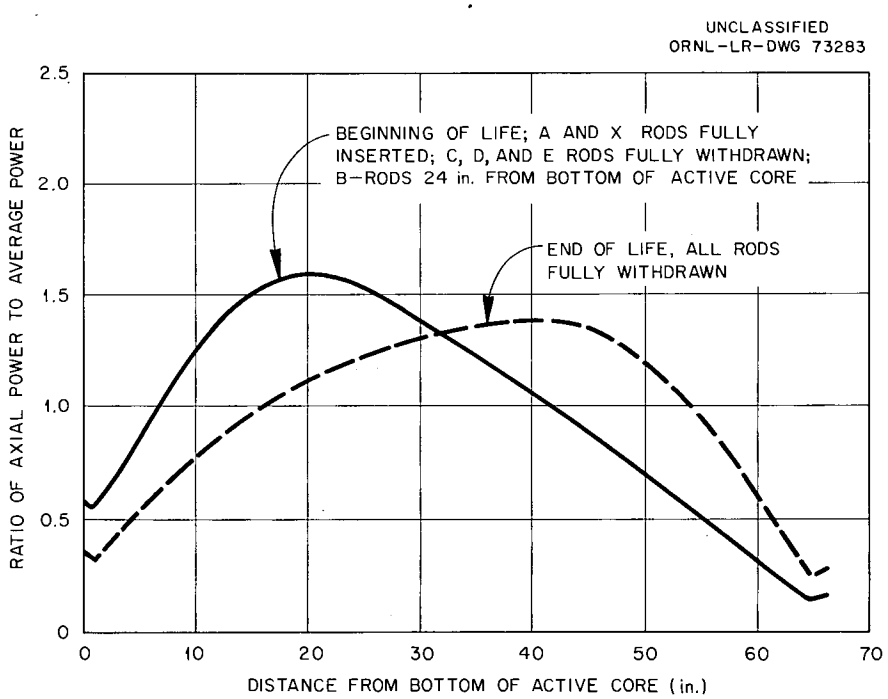

Fig. 23. Calculated Ratio of Axial Power to Average Power at Beginning and at End of Life for N.S. SAVANNAH Core I.

Table 4. Radial Power Peaking Factors for Various Rod Insertions in Core I at 508°F

Fully Inserted Rods	Radial Peak-to-Average Power Ratio	
	Two-Zone Core	One-Zone Core
No rods	1.98	2.05
X rod	1.60	1.65
A + X rods	1.44	1.48
A + B + X rods	1.49	1.48
All rods	1.44	1.70

that the most severe over-all power peaking occurs toward the end of core life when the X rod is almost fully withdrawn. At this point in core life, the over-all peak-to-average ratio obtained by simple combination of the axial window-shade results with the beginning-of-life radial peaking factor for no rods in the core is 2.9. This is considerably less than the design value[3] of 3.75. The peak-to-average power peaking factor obtained in the manner described above cannot account for true three-dimensional effects. It is estimated, however, from comparison of calculations with experimental results on the A-rod bank core I critical experiment (see sec. 8), that the method used here gives power peaking factors that are only about 10% lower than the experimental values. In addition, as shown by Figs. 12 and 13, it is expected that radial peaking factors should decrease with burnup.

10. WINDOW-SHADE BURNUP RESULTS FOR 4.2-WT % ENRICHED ZIRCALOY EGG-CRATE CORE

Core Life

Initial hot criticality conditions for the 4.2-wt % U^{235} Zircaloy egg-crate core require the X, A, and B rods to be fully inserted and the C, D, and E rods banked at 28 in. above the bottom of the active fuel. The rod-programming scheme followed in the window-shade burnup calculation was withdrawal of the C, D, and E rods as a unit, followed by withdrawal of B, A, and X rods in sequence, as in the stainless steel egg-crate calculations.

The resulting rod-movement history is displayed in Fig. 24. Again the resulting core life is in good agreement with the previous radial burnup calculation (Fig. 20) but gives a slightly longer lifetime estimate. Comparison of Figs. 21 and 24 again predicts that the replacement of stainless steel by Zircaloy in the fuel-element container structure will essentially double the reactivity lifetime of core I fuel elements.

Rod-bank worth curves for the Zircaloy egg-crate core are shown in Fig. 25. These curves are similar to the worth curves for a stainless steel egg-crate core shown in Fig. 22 and were obtained in the same manner. The clean, cold reactivity obtained by adding the worth of rods in the core is within $\Delta k = 0.002$ of the clean, cold reactivity of the core without any rods. Thus, the difference in lifetimes predicted by the radial and window-shade burnups cannot be ascribed to initial reactivity differences but is believed to be due to the more uniform fuel depletion attained in the window-shade calculation.

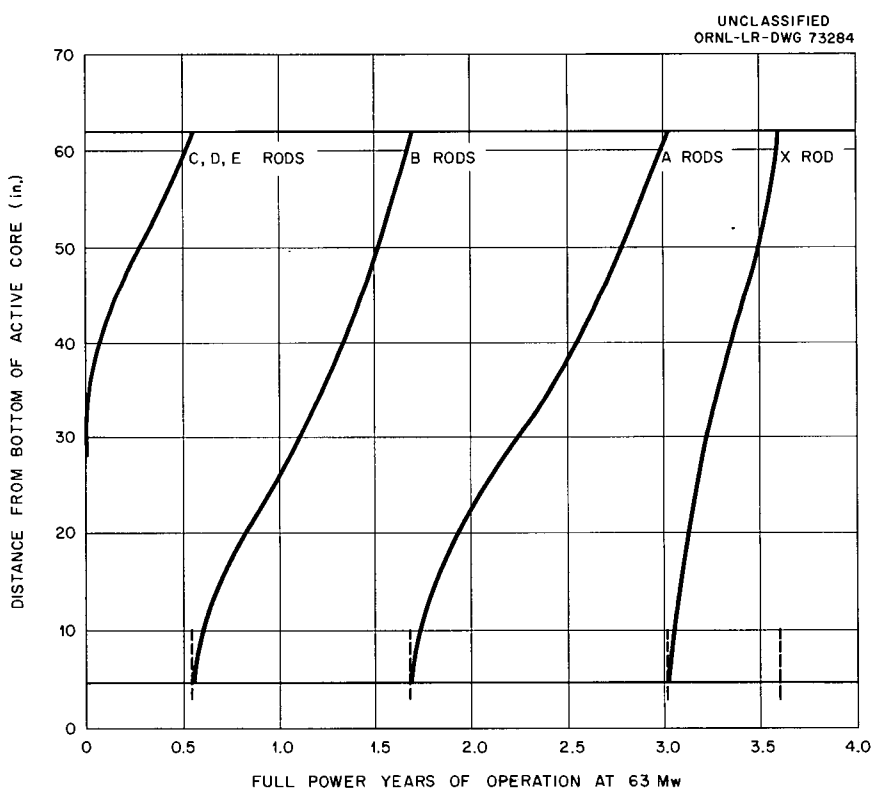

Fig. 24. Calculated Controlling Rod-Bank Position as a Function of Time for 4.2-wt % U^{235} Zircaloy Egg-Crate Core Operating at a Power Level of 63 Mw.

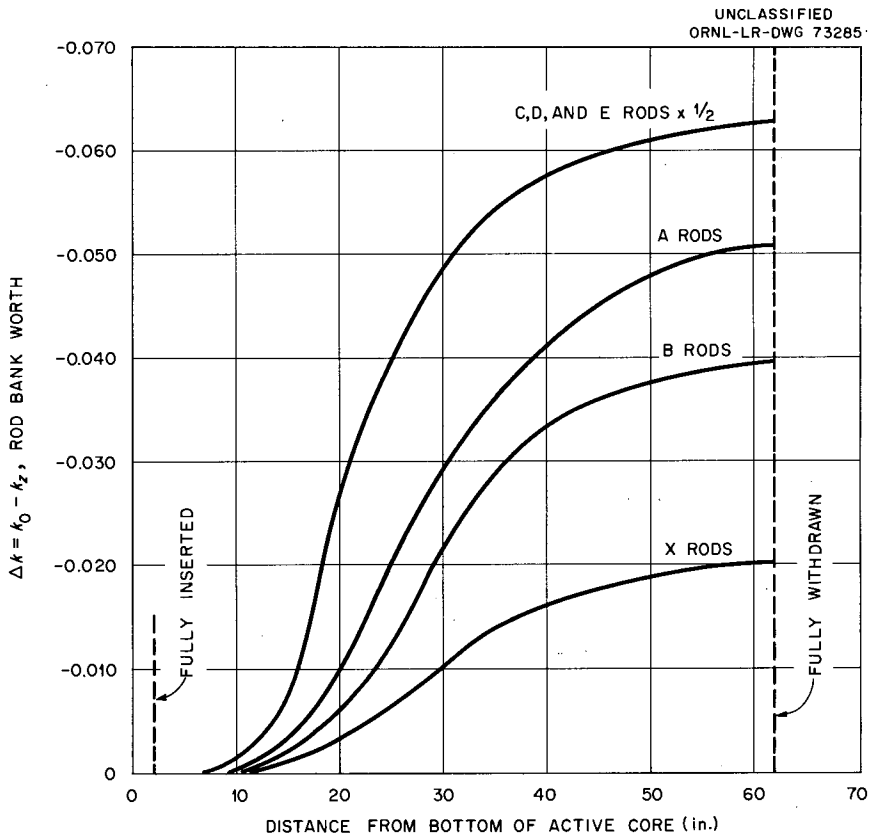

Fig. 25. Rod-Bank Worth as a Function of Bank Position Relative to the Fully Inserted Position for 4.2-wt % U^{235} Zircaloy Egg-Crate Core.

Axial Power Distributions

Beginning and end-of-life axial power distributions for the Zircaloy egg-crate core are shown in Fig. 26. Radial peaking factors for various rod configurations at 508°F are shown below:

Fully Inserted Rods	Radial Peak-to-Average Power Ratio
No rods	2.03
X rod	1.62
A + X rods	1.46
A + B + X rods	1.53
All rods	2.15

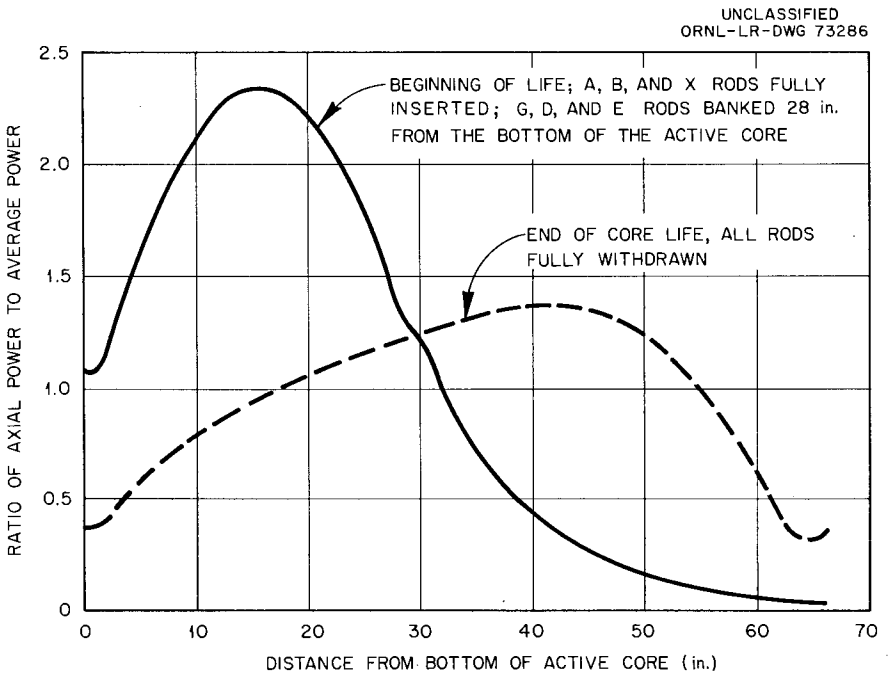

Fig. 26. Calculated Ratio of Axial Power to Average Power at Beginning and End of Life for 4.2-wt % U^{235} Zircaloy Egg-Crate Core.

The most severe power peaking occurs at the beginning of core life and has the value 3.55, which is lower than the design value of 3.75 but considerably higher than the maximum peaking factor of 2.9 in the stainless steel egg-crate core.

11. TEMPERATURE COEFFICIENT OF REACTIVITY

For a long-lived core such as would be obtained by the use of a Zircaloy egg crate and a fuel loading near 4.2 wt % U^{235}, there would usually be concern about the temperature coefficient of reactivity at full power for large plutonium inventories. The temperature coefficient of reactivity for a heterogeneous reactor of the N.S. SAVANNAH type depends a great deal on the core details; however, a determination of this quantity is beyond the scope of this work. Since plutonium is expected to affect only the moderator part of the over-all temperature coefficient reactivity, an estimate of the effect of plutonium on this part of the temperature coefficient could easily be made with the CANDLE code.

Such an estimate was made by changing the water density and thermal-group cross sections to their values for a 28°F temperature rise and recomputing multiplication factors at various times in core life using the radial CANDLE burnup calculation. Although this method cannot give absolute values for the moderator coefficient of reactivity, it should fairly well represent the effect of plutonium buildup on this coefficient. Using this method it was found that, although the buildup of plutonium does reduce the moderator coefficient, the percentage reduction is only about 10% after three years of full-power production.

Acknowledgment

We are indebted to Betty Maskewitz for adjusting the CANDLE code to meet our needs.

REFERENCES

1. E. E. Gross, B. W. Colston, and M. L. Winton, "Nuclear Analyses of the N.S. SAVANNAH Reactor with Zircaloy or Stainless Steel as Fuel-Element Containers," USAEC Report ORNL-3261, Oak Ridge National Laboratory, April 24, 1962.

2. C. L. Whitmarsh, "Potential Fuel-Cycle Cost Savings Resulting from Technological Changes in the N.S. SAVANNAH Reactor," USAEC Report ORNL-TM-144, Oak Ridge National Laboratory, April 6, 1962.

3. G. E. Kulynych, "Nuclear Merchant Ship Reactor, Final Safeguards Report, Description of the N.S. SAVANNAH," USAEC Report BAW-1164, Vol. I., Babcock & Wilcox Company, June 1960.

4. G. G. Bilodeau et al., "PDQ, An IBM-704 Code to Solve the Two Dimensional Few-Group Neutron-Diffusion Equations," USAEC Report WAPD-TM-70, Westinghouse Electric Company, 1957.

5. H. D. Brown, "Neutron Energy Spectra in Water," USAEC Report DP-64, E. I. DuPont de Nemours & Co., February 1956.

6. C. D. Petrie, M. L. Storm, and P. F. Zweifel, "Calculations of Thermal Group Constants for Mixtures Containing Hydrogen," Nucl. Sci. Eng., 2, 728 (1957).

7. C. L. Davis, J. M. Bookston, and B. E. Smith, "GNU, A Multigroup One-Dimensional Diffusion Program for the IBM-704," USAEC Report GMR-101, General Motors Corporation, November 12, 1957.

8. J. A. Thie, "A Simple Analytical Formulation of the Dancoff Correction," Nucl. Sci. Eng., 5, 75 (1959).

9. E. Hellstrand, "Measurements of the Effective Resonance Integral in Uranium Metal and Oxide in Different Geometries," J. Appl. Phys., 28, 1493 (1957).

10. R. L. Macklin and H. S. Pomerance, "Resonance Capture Integrals," p. 179 in Progress in Nuclear Energy, Series I, Physics and Mathematics, McGraw-Hill Co., Inc., New York, 1956.

11. D. J. Hughes and R. B. Schwartz, "Neutron Cross Sections," USAEC Report BNL-325, Brookhaven National Laboratory, July 1, 1958.

12. B. W. Colston, E. E. Gross, and M. L. Winton, "Heterogeneous Control-Rod Studies," p. 131 in Proceedings of the ANPP Reactor Analysis Seminar, MNDC-2487, January 1961.

13. B. G. Carlson and G. I. Bell, "Solution of the Transport Equation by the S_n Method," Proceedings of the Second United Nations International Conference on the Peaceful Uses of Atomic Energy, Geneva, 1958, Vol. 16, p. 535, United Nations, New York, 1958.

14. O. J. Marlowe and P. A. Ombrellaro, "CANDLE, A One-Dimensional Few-Group Depletion Code for the IBM-704," USAEC Report WAPD-TM-53, Westinghouse Electric Company, May 1957.

15. Oak Ridge National Laboratory, "Maritime Reactor Project Ann. Prog. Rep. Nov. 30, 1958," p. 34, USAEC Report ORNL-2657.

16. R. M. Ball, A. L. MacKinney, and J. H. Mortenson, "Marty Critical Experiments Summary of 4% Enriched UO_2 Cores for NMSR," USAEC Report BAW-1216, Babcock & Wilcox Company, May 1961.

17. E. A. Nephew, "Thermal and Resonance Absorption Cross Sections of U-233, U-235, and Pu-239 Fission Products," USAEC Report ORNL-2869, Oak Ridge National Laboratory, January 18, 1960.

18. R. M. Ball and A. L. MacKinney, "Nuclear Merchant Ship Reactor Zero Power Test, Core I," USAEC Report BAW-1202, Babcock & Wilcox Company, July 1960.

ORNL-3261, Suppl.

UC-80 — Reactor Technology
TID-4500 (18th ed., Rev.)

Internal Distribution

1. L. G. Alexander
2. F. S. Alsmiller
3. T. D. Anderson
4. V. E. Anderson (K-25)
5. C. D. Baumann
6. S. E. Beall
7. M. Bender
8. F. Binford
9. E. P. Blizard
10. A. L. Boch
11. R. B. Briggs
12. A. D. Callihan
13. R. S. Carlsmith
14. R. D. Cheverton
15. H. C. Claiborne
16. T. E. Cole
17. J. A. Conlin, Jr.
18. J. G. Delene
19. W. K. Ergen
20. A. P. Fraas
21. E. H. Gift
22-26. E. E. Gross
27. P. N. Haubenreich
28. V. O. Haynes
29. D. K. Holmes
30. W. H. Jordan
31. S. I. Kaplan
32. P. R. Kasten
33. W. E. Kinney
34. O. H. Klepper
35. R. B. Korsmeyer
36. J. A. Lane
37. C. E. Larson (K-25)
38. R. S. Livingston
39. T. S. Lundy
40. R. N. Lyon
41. H. G. MacPherson
42. F. C. Maienschein
43. W. D. Manly
44. E. R. Mann
45. J. H. Marable
46. B. F. Maskewitz (K-25)
47. H. C. McCurdy
48. J. T. Mihalczo
49. J. W. Miller (K-25)
50. F. H. Neill
51. L. Nelson
52. E. A. Nephew
53. C. W. Nestor, Jr.
54. A. M. Perry
55. P. H. Pitkanen
56. C. A. Preskitt
57. M. W. Rosenthal
58. T. H. Row
59. A. W. Savolainen
60. L. D. Schaffer
61. E. G. Silver
62. M. J. Skinner
63. J. A. Swartout
64. W. C. Thurber
65. M. L. Tobias
66. F. C. VonderLage
67. D. R. Vondy
68. A. M. Weinberg
69-71. M. L. Winton
72-75. ORNL-Y-12 Technical Library Document Reference Section
76-78. Central Research Library
79-103. Laboratory Records Department
104. Laboratory Records Department, R.C.

External Distribution

105. Ira Adler, New York Operations Office, AEC
106. Russ Aven, University of Mississippi
107. D. S. Beard, San Francisco Operations Office, AEC
108. Manson Benedict, Massachusetts Institute of Technology
109. R. F. Benenati, Brooklyn Polytechnic Institute
110. R. A. Charpie, UCC Research Administration, New York, N.Y.
111. B. W. Colston, Atomics International, Canoga Park, California
112-113. D. F. Cope, Reactor Division, AEC, ORO
114. C. M. Copenhaver, MITRE Corporation, Bedford, Mass.
115. D. E. Crouter, States Marine Lines, Inc., Camden, New Jersey
116. J. C. Ebersole, Tennessee Valley Authority, Oak Ridge, Tenn.
117. P. P. Eddy, General Electric Company, Atomic Equipment Department, San Jose, California
118. D. F. Fieno, National Aeronautics and Space Administration, Cleveland, Ohio
119. J. G. Gallagher, Westinghouse Corporation, Astronuclear Division, Pittsburgh, Pa.
120-121. W. C. Gribble, Division of Reactor Development (Army Reactors), AEC, Washington
122. Douglas C. MacMillan, George G. Sharp, Inc., New York, N.Y.
123-124. M. M. Mann, New York Shipbuilding Corporation, Camden, New Jersey
125-129. R. O. Mehann, States Marine Lines, Inc., Camden, New Jersey
130-131. L. J. Meisenheimer, Engineer Research and Development Laboratories, Fort Belvoir, Virginia
132. R. L. Murray, North Carolina State University
133-134. J. F. O'Brien, The Martin-Marietta Company, Nuclear Division, Baltimore, Maryland
135-144. J. E. Robb, Division of Reactor Development (Maritime Reactors), AEC, Washington
145. H. M. Roth, Research and Development Division, AEC, ORO
146-148. R. T. Schomer, The Babcock & Wilcox Company, Atomic Energy Division, Lynchburg, Virginia
149. R. S. Sevy, Atomics International, Canoga Park, California
150. D. H. Shaftman, Argonne National Laboratory
151. W. C. Stamm, Ebasco Services, Inc., New York
152. B. W. Winchell, Todd Shipyards Corporation, Nuclear Division, Galveston, Texas
153-759. Given distribution as shown in TID-4500 (18th ed., Rev.) under Reactor Technology Category (75 copies — OTS)